# FINITE ELEMENT ANALYSIS OF MULTILAYERED REINFORCED GRANULAR BED SOFT SOIL SYSTEM

A Thesis Submitted
in Partial Fulfillment of the Requirements
for the degree of

**Master of Technology**

*by*

Paritosh Kumar

to the

DEPARTMENT OF CIVIL ENGINEERING

INDIAN INSTITUTE OF TECHNOLOGY, KANPUR

JUNE, 2005

*DEDICATED*

*TO*

*MY PARENTS*

POST GRADUATE OFFICE
THESIS SUBMITTED
ON 24/6/06
I.I.T., KANPUR-2006

# CERTIFICATE

It is certified that the work contained in the thesis titled **"FINITE ELEMENT ANALYSIS OF MULTILAYERED REINFORCED GRANULAR BED SOFT SOIL SYSTEM"** by **Paritosh Kumar** (Roll No. Y3103031) has been carried out under my supervision and that this work has not been submitted elsewhere for a degree award.

Chandra

**Dr. Sarvesh Chandra**
Professor
Department of Civil Engineering
Indian Institute of Technology, Kanpur
Kanpur – 208016, India

# ABSTRACT

Name of student: Paritosh Kumar | Roll No: Y3103031

Degree for which submitted: M.Tech | Department: CE

Thesis Title: FINITE ELEMENT ANALYSIS OF MULTILAYERED REINFORCED GRANULAR BED SOFT SOIL SYSTEM

Name of thesis supervisor (s): Dr. Sarvesh Chandra

Month and Year of thesis submission: June, 2005

The present work pertains to multi layered reinforced earth foundation system and uses finite element analysis to predict the settlement response of foundation as well as reinforcements. Strip footing and combined footing resting on multilayer reinforced earth are considered for load acting at the centre and at the edges respectively. Reinforcements are placed evenly spaced in the dense compacted granular bed overlying loose soil deposit and one layer of reinforcement is placed at the interface between the loose soil layer and dense compacted granular bed. In this mechanical model foundation and reinforcements are modeled as one dimensional beam and soil is modeled as Winkler springs. Finite element formulation for foundation beam, reinforcing beam and soil are presented and elemental stiffness matrices for the same are obtained. The matrix equation in the final form is derived by assembling the elemental stiffness matrices and the load vectors and solved by Gauss elimination method after applying boundary conditions. The model results are validated by comparing it with closed form solution by Maheshwari (2004) in a degenerated case of one layer of reinforcement. A detailed parametric study for a range of non-dimensional parameters is carried out and the results are obtained for multilayer reinforced earth foundation system. It is found that increasing number of layers of reinforcement beyond three does not significantly contribute to the

settlement response of foundation beam. For three layers of reinforcements the reduction in maximum deflection of foundation beam are 23 % and 35 % for the load acting at the centre and at the edges respectively. Effects of various parameters on settlement responses of foundation and reinforcing beams for both loadings are found.

## ACKNOWLEDGEMENT

I take this opportunity to express my gratitude to my thesis adviser Prof. S. Chandra for his involvement, motivation and encouragement throughout this thesis work. The striking factor has been the freedom he gave me to work independently and his patient hearing with critical comments to this research problem.

I am grateful to Prof. P.K. Basudhar and Dr. N.R. Patra who have shown their interest throughout in this thesis work and queried about my work and suggested me time to time.

I thank the laboratory staffs for their help when I approached them for various purposes.

I thank all my classmates and friends especially Sarat Da, Kausik Da, Arindam, Shyam, Samresh and Subhatosh for their valuable suggestions and critical comments to complete this thesis work.

Finally I would like to express my gratitude to my parents and family members for their encouragement to do postgraduate studies and their support at all the times.

**Paritosh Kumar**

# CONTENTS

# LIST OF FIGURES

# LIST OF TABLES

# LIST OF SYMBOLS

Following symbols are used throughout this thesis unless otherwise specified.

| | |
|---|---|
| $y_1$ | Deflection of beams |
| $y_2$ | Deflection of reinforcing beam |
| $R_1$ | Characteristic length of foundation beam ($=\sqrt[4]{\frac{E_1 I_1}{k_1}}$) |
| $R_2$ | Characteristic length of Reinforcing beam ($=\sqrt[4]{\frac{E_2 I_2}{k_2}}$) |
| $R$ | Relative flexural rigidity of foundation beam and reinforcing beam ($=\frac{E_1 I_1}{E_2 I_2}$) |
| $r$ | Relative stiffness of the soil layers ($=\frac{k_1}{k_2}$) |
| $z_1$ | Non-dimensional length of foundation beam ($=\frac{l_1}{R_1}$) |
| $z_2$ | Non-dimensional length of reinforcing beam ($=\frac{l_2}{R_1}$) |
| $z_r$ | Ratio of non-dimensional length of beams ($z_r = \frac{z_2}{z_1}$) |
| $\gamma^{'}$ | Non-dimensional unit weight of upper layer of soil ($=\frac{\gamma R_1^2}{Q_t}$) |
| $h^{'}$ | Non-dimensional thickness of upper layer of soil ($=\frac{h}{R_1}$) |
| $z$ | Non-dimensional coordinate along the length of beams ($=\frac{X}{R_1}$) |
| $y_1^{'}$ | Non-dimensional deflection of foundation beam ($=\frac{y_1 E_1 I_1}{Q_t R_1^3}$) |
| $y_2^{'}$ | Non-dimensional deflection of reinforcing beam ($=\frac{y_2 E_2 I_2}{Q_t R_1^3}$) |
| $\{S\}^e$ | Double derivative of Hermitian shape functions ($=\frac{d^2\{N\}^e}{dx^2}$) |
| $\{S\}^{eT}$ | Transpose of $\{S\}^e$ |

| | |
|---|---|
| $[K_f]^e$ | Expanded elemental stiffness matrix of foundation beam |
| $[K_r]^e$ | Expanded elemental stiffness matrix of reinforced beam |
| $[Kk_t]^e$ | Expanded elemental stiffness matrix of top soil sub grade modulus |
| $[Kk_b]^e$ | Expanded elemental stiffness matrix of lower soil sub grade modulus. |
| $n_e^f$ | Number of elements of foundation beam. |
| $n_e^r$ | Number of elements of reinforcement beams. |
| $n_e^{k_1}$ | Number of elements of springs representing compact dense soil. |
| $n_e^{k_2}$ | Number of elements of springs representing poor soil. |
| $\left(\frac{du}{dx}\right)_i$ | The rotations of beam at global node i=1,2,3...*n*. |
| $\{F\}^e$ | Expanded load vector for beam elements. |
| $\{f\}^e$ | Elemental unexpanded load vector for beam elements. |
| $\{F_f\}^e$ | Expanded elemental load vector of foundation beam. |
| $\{F_r\}^e$ | Expanded elemental load vector of reinforcement beam. |
| $\{B\}^e$ | Vector contains derivative of Hermitian shape functions $(=\frac{d\{N\}^e}{d\xi})$ |
| $\xi$ | Natural co-ordinates |
| $u_1^e, u_2^e$ | Displacement degrees of freedom at the local nodes of a beam element |
| $\left(\frac{du}{dx}\right)_1^e, \left(\frac{du}{dx}\right)_2^e$ | Rotation degrees of freedoms at the local nodes of a beam element |

| | |
|---|---|
| $x_1^e, x_2^e$ | Co-ordinate of local node |
| $[C^b]$ | Connectivity matrix for beams |
| $[Ck^b]$ | Bottom spring connectivity matrix for loose soil |
| $[Ck^t]$ | Top springs connectivity matrix for compacted layer of soil |
| $[K]$ | Global stiffness matrix. |
| $[k]^e$ | Elemental stiffness matrix of beam element |
| $[k_G]^e$ | Geometric stiffness matrix for a beam element |
| $[k_s]$ | Elemental stiffness matrix for spring element |
| $\{B\}^{eT}$ | Transpose of $\{B\}^e$ |
| $\{F^*\}$ | Concentrated load vector |
| $\{F\}$ | Global load vector |
| $\{f\}^e$ | Elemental load vector of beam element |
| $\{N\}^e$ | Vector of Hermitian shape functions |
| $\mu$ | Coefficient of friction between reinforcement and surrounding soil |
| $b$ | Width of reinforcing beam |
| $C_{ep}, C_{eq}$ | Connectivity coefficients from connectivity matrices |
| $e$ | Element being considered |
| $E$ | Young's modulus of material of beam |
| $E_1I_1$ | Flexural rigidity of foundation beam |
| $E_2I_2$ | Flexural rigidity of reinforcing beam |
| $h$ | Thickness of upper layer of soil |

| | |
|---|---|
| $I_{zz}$ | Moment of area of section of beam |
| $k$ | Spring stiffness of soil |
| $k_1$ | Winkler spring stiffness of upper layer of strong soil |
| $k_2$ | Winkler spring stiffness of lower layer of poor soil |
| $k_{Gij}$ | Element of geometric stiffness matrix |
| $k_s$ | Subgrade modulus of soil |
| $l_1$ | Length of foundation beam |
| $l_2$ | Length of reinforcing beams |
| $l_e$ | Length of beam element |
| $M_{2i}$ | The concentrated moment at global node $i$ |
| $n$ | Number of global nodes |
| $nl$ | Number of layers of reinforcement |
| $p$, $q$ | Local node numbers to beam and spring elements used in assemblage to form global stiffness matrix |
| $Q$ | Concentrated load at centre of foundation beam |
| $Q_e$ | Concentrated load at the edges of foundation beam |
| $Q_t$ | Normalizing parameter for normalizing deflections represents load |
| $r$, $s$ | Position indices in global matrices |
| $u_i$ | Displacements of beam at global node i =1,2,3…$n$ |
| $W_{2i-1}$ | Concentrated forces in concentrated load vector |

| | |
|---|---|
| $W_{2i-1}$ | The concentrated force at global node $i$ |
| $W_e$ | External work done |
| $W_{\mathrm{i}}$ | Internal work done |
| $\gamma_1$ | Unit weight of dense compacted layer of soil |
| $\gamma_2$ | Unit weight of loose soil layer |

# CHAPTER 1

# INTRODUCTION

## 1.1 General

With the rapid development of infrastructure in the present era there is an increased demand for land. Scarcity of good land and their exorbitant cost forced the developers to construct on the poor soils having low supporting capacity giving birth to the development of a new area called ground engineering. One of the ground improvement techniques is reinforcing the poor soil with inclusion of reinforcing material e.g. bamboo strip, ropes, metal strips, geosynthetics etc. to create a composite material with improved performance characteristics. The use of geosynthetics for soil reinforcement is very extensive and increasing annually. The simplicity of the basic principles of geosynthetic reinforcements and the economic factors over the conventional approach makes it very attractive to the civil engineers. A large number of experimental and analytical studies have been carried out in the last three decades in the area of footings resting on soil reinforced with geosynthetic reinforcement. The analysis of the interaction between structural foundations and supporting soil media is of fundamental importance to geotechnical engineering. Results of such analyses provide information, which can be used in the design of foundations and in the analysis of stresses and deformations within the supporting soil medium. Various analytical, numerical and experimental methods are used for the analysis of foundations on reinforced ground. This present study analyzes the foundation beams resting on earth reinforced with multilayer geosynthetic reinforcement by finite element method with lumped parameter approach for the settlement response of foundation beam and reinforcements.

## 1.2 Scope and organization of the present work

A brief review of theoretical works on the behavior of foundations on reinforced soil is presented with conclusive remarks in chapter 2.

From the review of the literature, it has been observed that a very few works have been done on reinforced earth foundation system taking into consideration the bending stiffness of reinforcement either for single layer reinforcement or for multi-layer reinforcement. Thus it is felt that there is a need to undertake such a study and the same is presented in the following chapters.

Problem formulation and method of analysis is presented in chapter 3. In this chapter statement of the problem is presented. The formulation for foundation beam, reinforcing beam, soil and the effect of frictional force and prestressing force in beam in finite element form is presented subsequently.

Results and discussions of the present study are presented in chapter 4. Effects of various parameters on the settlement behavior of the foundation and reinforcement are discussed.

Chapter 5 deals with the conclusions of the present study and finally future scope of the present work is presented.

# CHAPTER 2

# LITERATURE REVIEW

## 2.1 General

Ground improvement techniques are one of the most interesting and widely studied topics in geotechnical engineering. Reinforcement of soft soils to improve the bearing capacity and reduce settlements of structures built on them is a very efficient method and is becoming increasingly common. Geosynthetic reinforcements have been proved to be very efficient and cost effective in ground reinforcement. There has been a need to study the geosynthetic reinforced soil foundations to predict the behavior of foundation and soil. Several studies have been done on the geosynthetic-reinforced earth in the past three decades to find the effective use of such foundation systems. The brief review given in the following section refers to the literature related to the theoretical works carried out in the area of reinforced earth to study the response of the foundation on reinforced soils.

## 2.2 Geosynthetic reinforced soil foundation system

Binquet & Lee (1975) analyzed the bearing capacity problem of a surface strip footing on a granular soil reinforced with horizontal layers of tensile reinforcement. The failure surface was determined as the locus of the points of maximum shear stress at different depth based on the elastic theory of stresses i.e. by applying the Boussinesq equation. It was arbitrarily assumed that the tie force per layer varies inversely with the number of layers, $N$ in the foundation due to lack of definitive data. Idealized approximate cost analysis indicated that if corrosion was neglected, savings up to 100% can be considered over the cost of conventional foundation. As

Boussinesq equation was found to be unsatisfactory for determining stresses in the case of the foundation on granular soil overlying a finite sized pocket of soft material, linear elastic finite element program was used for the analysis.

Brown & Poulos (1981) presented an analytical model to investigate the increase in bearing capacity and stiffness of a foundation due to the placement of reinforcement in the homogeneous soil layer, and soil bed overlying a cavity. The analysis considered various components of the reinforced soil separately and incorporated an elasto-plastic Mohr-Coulomb failure criterion, equivalent-width elastic reinforcement strips with zero flexural rigidity transmitting axial forces only, and a model for reinforcement-soil bonding which allowed for slippage governed by Mohr-Coulomb failure criterion. It was concluded that the improvement of the performance characteristics of the reinforced soil bed depended both on the number of reinforcing layers and also on the concentration (surface area per unit width of the footing) of the reinforcement, the latter being the major dominant factor as it was observed that the limit state of the reinforcement-soil bond was reached at an early stage. However, the study was only conducted for four layers of reinforcement due to lack of resources and thus needed further investigation about the effect of number of reinforcing layers on the performance characteristics of the reinforced soil bed.

Andrawes et al. (1982) analyzed soil-geotextile systems by using finite element method. They described the nature of the elements used to represent the soil-geotextile systems for the purpose of predicting the stress-strain behavior. Studies were done with a footing resting on dense sand without or with geotextile placed at various depths. It was observed that if the soil properties could be correctly represented in the soil elements, good correlations up to 85% were obtained between

predicted and measured data. However, it was suggested that the finite element method was inappropriate for the soils in which local failures occur.

Madhav & Poorooshasb (1988) proposed a new foundation model element – the rough membrane to represent the response of the geofabric. Combining this element with the Winkler springs and Pasternak shear layers to model respectively the soft soil and granular fills, the foundation model was proposed for geosynthetic-granular fill-soft soil system. Analysis of results at small displacement indicated the effect of granular fill to be more significant than that of the membrane. It was also observed that the effect of membrane increased with the load or decreasing soil stiffness.

Poran et al. (1989) presented a design procedure based on finite element analysis, which included a visco-plastic model for soils and special visco-elastic membrane elements to model geogrid behavior. It was suggested that the footing settlement is the governing design criteria, and therefore granular layer thickness and footing size should be determined based on allowable settlement, especially with geogrid reinforcement. The proposed design procedure for continuous and axisymmetrical footing was especially beneficial where small settlements were encountered.

Ghosh & Madhav (1994a) developed a simple mathematical model to account for the membrane effect of a reinforcement layer on the load settlement response of a granular fill-soft soil foundation system. The nonlinear loading pressure-settlement response of the granular fill and soft soil, respectively, for the plane strain condition were incorporated in the formulation. Parametric studies for a uniformly loaded strip footing showed that the membrane action of reinforcement caused reduction in the settlement below the footing which is over and above the settlement due to granular

fill. The type of foundation considered consisted of a layer of frictional fill over soft clay. In the reinforced case, the reinforcement was placed within the granular fill and at the fill-clay interface. The normal stresses at the reinforcement interfaces were not much affected by their presence and the internal stability of the reinforced soil system might be impaired by the tensile rupture of the reinforcement or by lack of adherence of the soil at the reinforcement interface. However, in the reinforced case, analysis with multi-layer of reinforcement was not undertaken. It was observed that the settlement behavior significantly improved with respect to the stiffness of granular fill, when the soil was softer, and with respect to the interfacial friction, when the fill material was stiff.

Ghosh and Madhav (1994 b) developed a mathematical model for the analysis of a reinforced foundation bed by incorporating the confinement effect of a single layer of reinforcement. It was quantified in terms of the average increase in confining pressure due to the reinforcement from which modified shear stiffnesses of the granular soil surrounding the reinforcement were obtained. The parametric studies were sensitive to the methods used for obtaining the modified shear stiffness of granular fill. The confinement effect was more pronounced when the shear stiffness of the granular fill was large. The modified shear stiffness below the centre of the footing increased by two to five times the initial values of shear stiffness.

Ghosh and Madhav (1994 c) proposed a new model for a reinforced shallow foundation bed by incorporating the 'rough membrane' element for single layer reinforcement. Mechanics of the rough membrane element with the assumption of horizontal shear stress transfer at the soil/reinforcement interfaces were explained and formulated. The model was generalized by incorporating nonlinear response of the soft soil and of the granular fill under plane strain loading conditions. The membrane

effect was quantified in terms of the improvement in the load-settlement responses of the composite foundation system over the unreinforced one. Parametric studies indicated that reinforcement while in tension spreads the load over a larger area, leading to a reduction in the settlement beneath the footing.

Shukla & Chandra (1994a) studied the effect of prestressing the geosynthetic reinforcement on the settlement behavior of geosynthetic-reinforced granular fill-soft soil system. The foundation model element had a prestressed rough membrane embedded in a granular layer. Parametric studies revealed that the settlement reductions within the loaded regions were observed even for low prestress in the reinforcement. It was observed that the improvement in settlement response increased with the increase in prestress in the geosynthetic reinforcement within the loaded region and was most significant at the centre of the loaded footing, which reduced differential settlement. On soft soils or at higher load intensities more prestress was required in the geosynthetic reinforcement to achieve a particular settlement reduction compared with stiff soils or lower load intensities. The influence of Prestressing increased with the width of the reinforced zone up to $L/B$ ratio of 2.0. The effect of prestressing was significant at lower values of shear parameter of granular fill and interface friction coefficients at top and bottom of geosynthetic reinforcement. It was also observed that the mobilized tensile force in the geosynthetic layer increased at all locations with the increase in prestress but the increase was maximum at the edges of the footing. It was concluded that prestressing the geosynthetic reinforcement was a significant ground improvement technique to enhance the settlement characteristics of the soft soils where the membrane effect of reinforcement is required.

Shukla & Chandra (1994b) proposed a foundation model to incorporate compressibility of the granular fill by attaching a layer of Winkler springs to the

Pasternak shear layer. The effect of compaction of granular fill in terms of lateral stress ratio was also considered. The parametric studies indicated that the consideration of the compressibility of the granular fill resulted in a significant increase in the settlement of the reinforced foundation soil. The model used was fairly general in nature as it accounted for the compressibility of the granular layer, in addition to the effects of prestressing of geosynthetic reinforcement and overconsolidation (through compaction) of the granular fill. The model was capable of incorporating the effect of any degree of compressibility of the granular fill by proper selection of its modulus of subgrade reaction. Finite Difference scheme was employed to produce the numerical solution. Non-dimensionalized results were produced for practical applications. The effect of the compressibility of the granular fill on the load settlement characteristics of geosynthetic-reinforced granular fill-soft soil system was observed to be significant at all the load intensities except for very small values of the load. With the increase in the compressibility of the granular fill, the order of increase in the settlement was more at the edges than in the centre of the loaded region. For any degree of compressibility of granular fill, the geosynthetic-reinforced granular fill-soft soil system behaved as much as a stiffer system at higher load intensities. The order of increase in the settlement with increase in the compressibility of the granular fill at any location within the loaded region was greater for lower values of shear parameter.

Shukla & Chandra (1994c) described a mechanical model for idealizing the settlement response of a geosynthetic-reinforced compressible fill-soft soil system, by representing each subsystem by commonly used mechanical elements such as stretched, rough, elastic membrane, Pasternak shear layer, Winkler springs and dashpot. The model considered simultaneously several factors governing its behavior

such as the compressibility of the granular fill, the time-dependent behavior of soft soil and prestress in the geosynthetic reinforcement, besides the material and soil-geosynthetic interface characteristics. The response function of the model had been derived for strip loading in plane strain conditions. The resulting equations, in nondimensional form were solved by an iterative finite difference method. It was observed that the compressibility of the granular fill had an appreciable influence on the settlement response of the geosynthetic-reinforced granular fill-soft sol system as long as the stiffness of the granular fill was less than approximately 50 times that of soft soil. It was also concluded that the pre-stressing of the geosynthetic reinforcement and the compaction of the granular fill resulted in the settlement reduction of reinforced fill-soft soil system.

Gharpure (1995) studied the finite element analysis of geotextile reinforced sand bed subjected to strip loading. The soil was modeled as plain strain element and reinforcement as one dimensional line element with zero thickness. The confinement and string effect of reinforcement was considered along with the slip between geotextile and surrounding soil and gave the optimum depth of placement for geotextile.

Yin (1997) proposed a new one-dimensional mathematical model for modeling geosynthetic-reinforced granular fills over soft soils subjected to a vertical surcharge load. The geosynthetic reinforcement consisted of a membrane (geogrid, or geotextile) placed horizontally in engineered granular fill, which was constructed over a soft soil. The proposed model was mainly based on the assumption of a Pasternak shear layer. A new approach consisted of incorporating a deformation compatibility condition into the model. The compatibility condition eliminated the need for two uncertain model parameters that were required to calculate the shear stresses between

the top and bottom granular fill layers and the geosynthetic layer. The compatibility condition also provided the possibility to include the geosynthetic stiffness in the model. Comparisons were made with a two-dimensional finite element model and three other one-dimensional models. The proposed model could also consider the nonlinear and elastic-plastic behavior of the granular fill.

Yin (2000) performed a study of reinforced beam on elastic foundation. Governing ordinary differential equations were derived for a reinforced Timoshenko beam on an elastic foundation. An analytical solution was obtained for a point load on an infinite Timoshenko beam (TB) on elastic foundation. Special attention was drawn to the location, tension, and shear stiffness of reinforcement and its influence on settlement/deflection of the beam and reinforcement tension force. The TB model was suggested to be particularly useful in modeling a reinforced beam with or without considering the reinforcement shear stiffness. Practical applications of the TB model were recommended in modeling geosynthetics/fiber-glass reinforcement of foundation or pavement. A finite element (FE) model was established for the same infinite beam problem. Comparisons were made with the FE model and PB model (Winkler model based on pure bending theory). It was observed that the TB model generally predicted larger settlement and less tension force in the distance at or near the point load, as compared to the PB model. However, comparable results were obtained with the FE model. It was suggested that the TB model was superior to the Winkler model in considering the shear deformation of the beam and the reinforcement. The TB model could consider the shear stiffness of reinforcement, especially for the geosynthetics, which have almost zero shear stiffness due to very thin thickness. However, the TB model suffered from the same limitations as that of

the Winkler model. The TB model also suffered from the limitation due to the assumption of zero vertical strain on the beam.

Fakher and Jones (2001) presented a numerical simulation to model a layer of sand overlying a layer of geosynthetic reinforcement and super soft clay. It was suggested that bending stiffness should be considered while having earthworks on super soft clay. It was suggested that the structural behavior of the reinforcement over super soft clay was like a stiff plate supported by the vertical reaction force from the clay. If the plate is anchored horizontally, it will present a high resistance to the vertical load. The effect of the reinforcement pullout resistance was to provide a horizontal restraint for the plate. It was concluded that the higher the reinforcement bending stiffness, the higher the bearing capacity of the system. It was observed that the reinforcement with high bending stiffness reduced the surface heave, which was distributed over a wider area. With very stiff reinforcement, the maximum heave did not occur at the surface. The relative importance of the bending stiffness of the reinforcement was observed to be in particular cases. When the ratio of depth of placement of reinforcement to the footing width is small, the increase of the bearing capacity ratio due to the bending stiffness is significant. When the footing width increases, the effect of bending stiffness decreased sharply. It was concluded that the bending stiffness was not important unless the underlying clay layer was not in a super soft state.

Maheshwari (2004) analyzed a model to predict the flexural response of beam resting on dense compacted soil overlying loose soil deposit with one layer of geosynthetic reinforcement such as geogrids at the interface of soil layers. Both the foundation and reinforcement were idealized as beams with smooth surface characteristics. The lower poor strata and upper dense soil were modeled using

Winkler springs of different stiffness. Effect of the depth of placement of reinforcement was considered by taking surcharge on reinforcement. The governing differential equations for the response of the beams were derived and closed-form were obtained subjected to appropriate boundary and continuity conditions. The model results showed very good agreement with the solution provided by Hetenyi for infinite beams on elastic foundation in a particular case. Practically no change was observed in the normalized deflection of the upper and lower beams when the normalized length ratio of beams exceeded 1.5 for the range of parameters considered. The normalized depth of placement of the lower beam had a significant effect on the deflection profile of both foundation and reinforcing beams. The maximum normalized deflection of the upper and lower beam increased by 37% and 45% respectively as the normalized depth increases from 0.5 to 1.5 for load acting at the centre of foundation beam. For loads acting at the edges of foundation beam the maximum normalized deflection of the upper and lower beam increased by 14-15 % and 25% respectively as normalized depth increases from 0.5 to 1.5. The relative flexural rigidity of the beam, $R$ affected the deflection at the edges of the beam more than at the centre. The maximum normalized deflection of the upper beam decreased by 11% as $R$ increases from 50 to 1 while for lower beams it decreased 55% for a reduction of $R$ from 50 to 1. The relative stiffness of soils, $r$, had a significant influence on the normalized deflection of upper and lower beam. The maximum normalized deflection decreases by 84 - 85 % and 32 – 33 % for upper and lower beam respectively as r decreases from 20 to 1.The load acting on foundation beam had a significant influence on the deflection of beams. The normalized deflection of the beams could be reduced to the extent of 70-75% at the centre and by more than 95% at the edges of the beams.

## 2.3 Motivation of present work

From the review of literature, it is noticed that a few studies have been carried out on reinforced earth foundation system taking bending stiffness of reinforcement in to consideration. First Fakher and Jones (2001) considered the bending stiffness of geosynthetic reinforcement and concluded that bending stiffness of reinforcement has significant influence on the bearing capacity of the reinforced earth. Maheshwari (2004) have also considered the bending stiffness of reinforcement and analyzed the foundation beam on reinforced soil with one layer of reinforcement and gave the close form solution for the settlement response of foundation and reinforcement. The present study is an extension of the work done by Maheshwari (2004) for multilayer reinforcement and FEM is chosen as method of analysis to predict the settlement response of foundation as well as reinforcements.

# CHAPTER 3

# PROBLEM FORMULATION AND METHOD OF ANALYSIS

## 3.1 General

Finite Element Method (FEM) is well recognized as a very powerful and versatile numerical tool for solving stress-strain and displacement related problems. FEM is specially suited for continuum problems like modeling of soil, but it is also well suited and accurate with lumped parameter approach, if parameters and size of elements are properly chosen and are well organized. In this thesis lumped parameter approach is followed. From the review of literature in chapter 2 it is observed that reinforcements like geogrids and geocells may have bending stiffness also. Maheshwari (2004) modeled foundation and reinforcement as beam and considered one layer of reinforcement at the interface between the dense compacted granular bed and loose soil deposit and gave close form solution for the settlement response of foundation as well as reinforcement. In the present study the work done by Maheshwari (2004) is extended for multilayer reinforcement and FEM is chosen as method of analysis to predict the settlement response of foundation and reinforcements. Statement of the problem is presented first then in the following sections, the finite element formulations for foundation beam, reinforcing beam and soil are presented and elemental stiffness matrices are formed for the same. Friction and prestress in reinforcement beam are treated as axial force in beam and the formulation is given for the same. Then the finite element mesh details and connectivity of the

various components are discussed. Finally assemblage of elemental stiffness matrices and load vectors to derive finite element equation in matrix form, application of boundary conditions and solution of FEM equation are described.

## 3.2 Statement of the problem

The cases of strip footing of length $2l_1$ acted up on by a concentrated load $Q_t$ at the centre is shown in Fig. 3.1 (a) and a combined footing of length $2l_1$ acted upon by concentrated load $Q_t$ at the edges is shown in Fig. 3.1 (b). Footings are idealized as elastic beams with flexural rigidity $E_1I_1$ resting on dense compacted soil of depth $h$ placed over loose soil deposit. Geosynthetic reinforcements (geogrids or geocells) are idealized as beams of length $2l_2$ with flexural rigidity $E_2I_2$ and are placed at the interface of soil layers as well as in dense compacted soil layer with equal spacing h/3 as shown in Fig. 3.1 (a) and 3.1 (b) for strip footing and combined footing respectively (Figs. are drawn for three layers of reinforcements for simplicity). The strong soil layer and underlying poor soil are idealized as Winkler springs of stiffness $k_1$ and $k_2$. The unit weights of upper and lower layer of soil are $\gamma_1$ and $\gamma_2$ respectively. Fig. 3.2 shows the idealized model of above described reinforced earth foundation systems, which represents strip footing by considering the load Qt at the centre, and combined footing can be represented if the loads $Q_t$ are considered at the edges. The prestess force in foundation beam is $T_f$ and prestress in reinforcing beams are $T_1$, $T_2$, and $T_3$ for layer - 1 layer - 2 and layer - 3 respectively and these forces are zero in absence of prestress forces. In this present study foundation beam is assumed to be smooth and frictional forces of tensile nature are developed in the reinforcing beam resulting from interfacial friction between reinforcing beam and surrounding (shown in Fig. 3.2). Loading on foundation beam is assumed to be symmetric and valid for strip footing and combined footing.

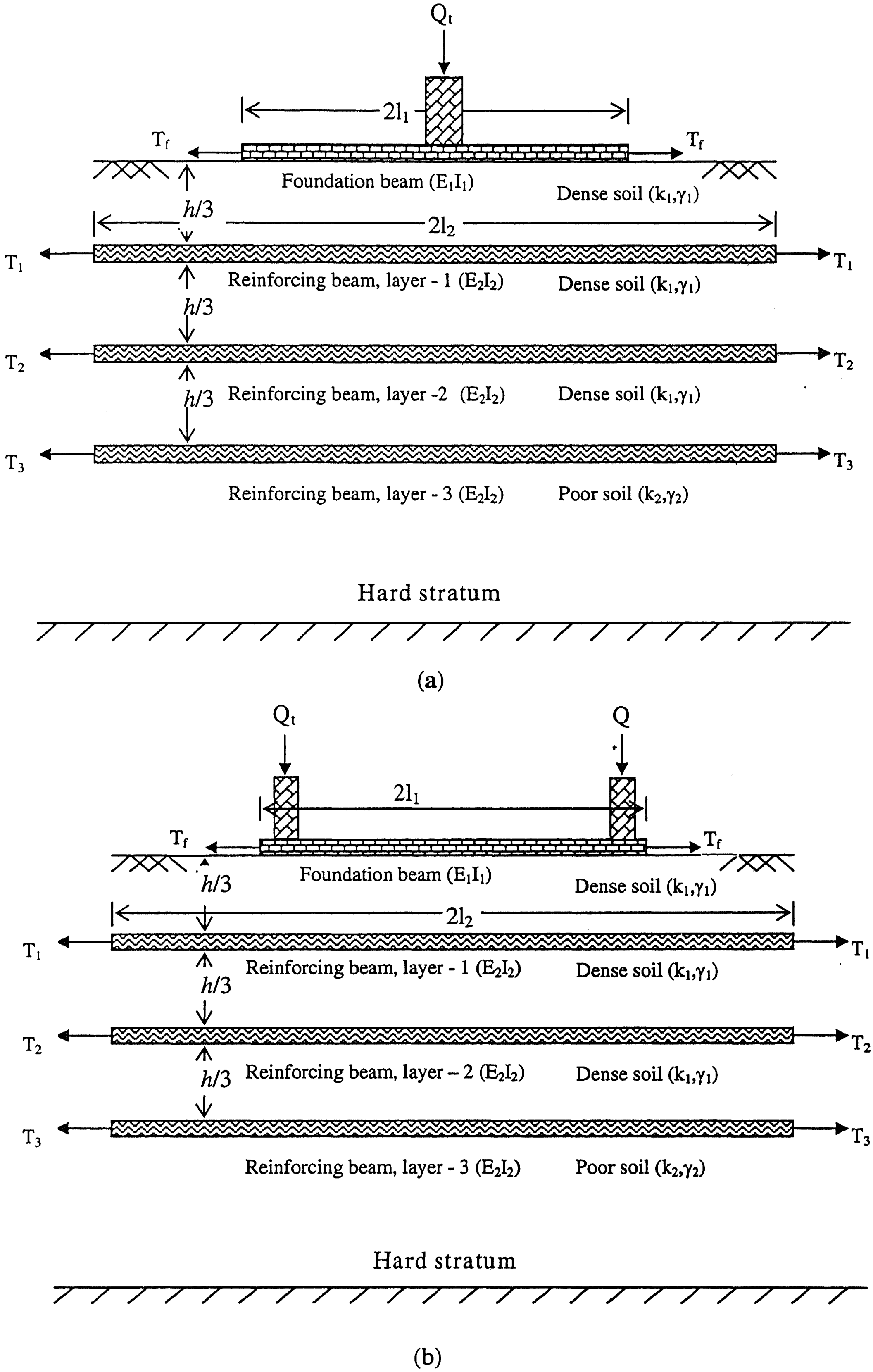


**Fig. 3.1: Definition sketch of the problem: (a) strip footing, (b) combined footing**

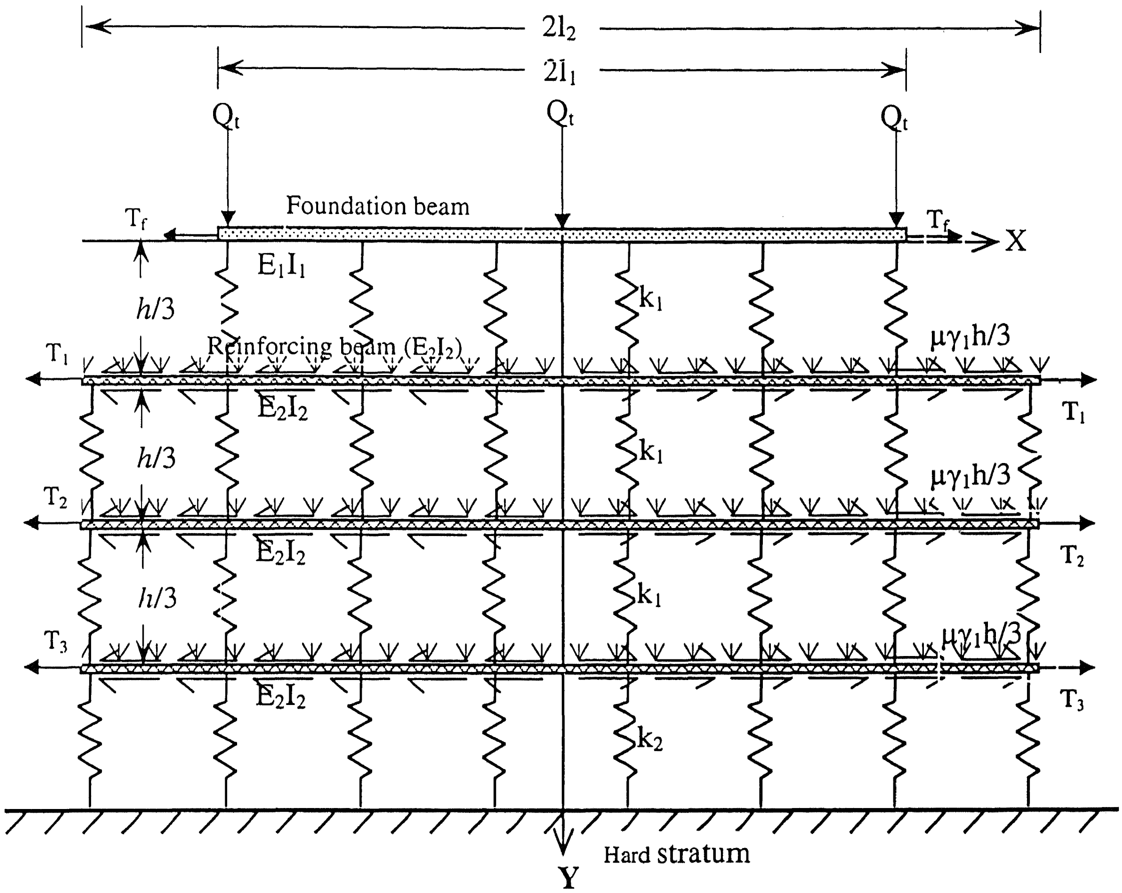


**Fig. 3.2: Idealization of the problem**

## 3.1 Formulation of foundation and reinforcing beams

Foundation and reinforcement beams are modeled as a typical two noded one dimensional beam element. Displacement $u$ and rotation $\frac{du}{dx}$ are considered as degrees of freedom at each node as shown in Fig. 3.3. Stiffness matrix for such beam element is well established and is used in the present study. In this section formulation for a typical one dimensional beam element (as shown in Fig.3.3) is presented. All equations in this section are taken from Tirupathin et al. (2003).

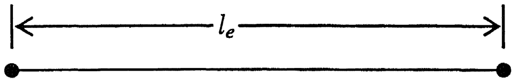


| | | |
|---|---|---|
| 1 | 2 | : Local node |
| $u_1^e, \left(\dfrac{du}{dx}\right)_1^e$ | $u_2^e, \left(\dfrac{du}{dx}\right)_2^e$ | : Elemental degrees of freedom |
| $x_1^e$ | $x_2^e$ | : Coordinate of local node |
| $-1 = \xi_1$ | $1 = \xi_2$ | : Natural coordinates of local nodes |

**Fig. 3.3: A typical beam element**

### 3.3.1 Elemental beam stiffness matrix

Elemental stiffness matrix for the beam element shown in Fig. 3.3 is given as

$$[k]^e = \int_{x_1^e}^{x_2^e} \left[ EI_{zz} \{S\}^e \{S\}^{eT} \right] dx \tag{3.1}$$

where

$[k]^e$ is the elemental stiffness matrix for the considered element '*e*'.

$$\{S\}^e = \frac{d^2\{N\}^e}{dx^2} \tag{3.2}$$

$\{S\}^e$ is the row vector contains the derivatives of Hermitian shape functions $\{N\}^e$ in local x coordinate.

$E$ is Young's modulus of elasticity of the considered element.

$I_{zz}$ is moment of area of the considered element.

$\{S\}^{eT}$ is the transpose of $\{S\}^e$.

### 3.3.2 Numerical Integration for obtaining elemental stiffness matrix

To numerically integrate the equation (3.1), equation is first converted to natural coordinates and then it is integrated by Gauss quadrature numerical integration scheme as given below.

Equation (3.1) is converted in natural coordinate as

$$[k]^e = \int_{x_1^e}^{x_2^e} \left[ \frac{8EI_{zz}}{l^{e^3}} \{S\}^e \{S\}^{eT} \right] d\xi \tag{3.3}$$

Gauss quadrature numerical integration scheme is

$$[k]^e = \sum_{m=1}^{n_g} w_m \left( \frac{8E^e I^e{}_{zz}}{l_e^3} \{S\}^e \{S\}^{eT} \right)_{\xi=\xi_m} \tag{3.4}$$

where,

$n_g$ is number of gauss points used.

Gauss points used are -0.577350269189626, 0.577350269189626.

$W_m$ is the weight corresponding to gauss points are1.0, 1.0.

$$l_e = x_2^e - x_1^e \tag{3.5}$$

$$E^e = \sum_{i=1}^{2} L_i^e E_i^e \tag{3.6}$$

$$I_{zz}^e = \sum_{i=1}^{2} L_i^e I_i^e \tag{3.7}$$

where $L_i^e$ are Lagrangian shape function in natural coordinates for nodes i = 1, 2 for typical element '*e*' is given as

$$L_i^e(\xi) = \frac{\prod\limits_{\substack{j=1\\ j\neq i}}^{2} (\xi - \xi_j)}{\prod\limits_{\substack{j=1\\ j\neq i}}^{2} (\xi_i - \xi_j)} \tag{3.8}$$

Shape function derivatives are given as $\{S\}^e = \dfrac{d^2\{N\}^e}{d\xi^2}$ (3.9)

where,

Hermitian shape functions in natural coordinates $\{N\}^e$ are given as:

$$N_{2i-1}^e = \left[1 - 2(\xi - \xi_i^e)\left(\frac{dL_i}{d\xi}\right)\Big|\xi = \xi_i\right]L_i^2 \tag{3.10}$$

$$N_{2i}^e = \frac{l_e}{2}(\xi - \xi_i)L_i^2 \tag{3.11}$$

where

$L_i$ are Lagrangian shape functions for nodes $i = 1, 2$ of element $e$.

$l_e$ is length of beam element.

Shape function derivatives $S^e = \dfrac{d^2\{N\}^e}{d\xi^2}$ in natural coordinate scheme are

$$S_1^e = \frac{1}{4}(6\xi)$$

$$S_2^e = \frac{l_e}{8}(-2 + 6\xi)$$

$$S_3^e = \frac{1}{4}(-6\xi)$$

$$S_4^e = \frac{l_e}{8}(2 + 6\xi)$$

## 3.4 Formulation of soil

Soil is modeled by Winkler springs and is found to be very effective in lumped parameter approach. In this section elemental stiffness matrix for soil element is found. A typical two noded line element is chosen for Winkler spring as shown in Fig. 3.4. Displacements at nodes ($u$) are considered as degree of freedom for the spring element. Since each node have two degrees of freedom displacement ($u$) and rotation $\left(\frac{du}{dx}\right)$ for the foundation and reinforcing beams, in elemental stiffness matrix for spring element, elements are present only on displacement fields, and it contains zeros corresponding to rotation fields.

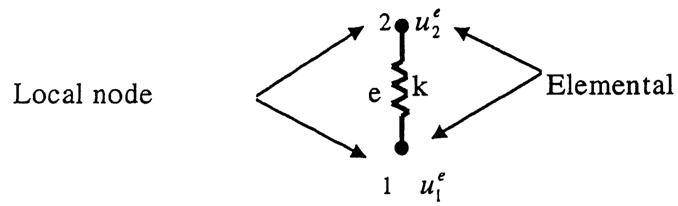


**Fig. 3.4: A typical spring element**

Spring stiffness $k$ is taken as, $k = k_s \times l_e \times b$

Where, $k_s$ is subgrade modulus, $l_e$ is length of beam element and $b$ is the width of beam.

A typical elemental stiffness matrix for spring element is given as

$$[k_s] = \begin{bmatrix} k & 0 & -k & 0 \\ 0 & 0 & 0 & 0 \\ -k & 0 & k & 0 \\ 0 & 0 & 0 & 0 \end{bmatrix}$$

where, $k$ represents the spring stiffness of corresponding soil.

## 3.5 Formulation for the effect of prestress force and friction force

In this thesis, prestress and frictional forces are considered as axial force in foundation and reinforcement. As foundation and reinforcement are modeled as beam, prestress and friction effect are modeled as beam with axial force. All the equations given in this section are taken from Clough and Penzien (1993). When a beam element is subjected to an axial force, the modification is made to stiffness coefficient $K_{ij}$ by geometric stiffness $k_{Gij}$, which is defined as the force corresponding to nodal coordinate $i$ due to a unit displacement at coordinate $j$ and resulting from the axial forces in the structure. These coefficients are evaluated by application of principle of virtual work. Consider a beam as shown in fig. 3.3 but now subjected to a distributed axial force per unit of length $P_a(x)$, as shown in Fig. 3.5 (a). In the sketch in Fig. 3.5 (b), the beam segment is subjected to a unit rotation at the left end, $\left(\dfrac{du}{dx}\right)_1^e = 1$.

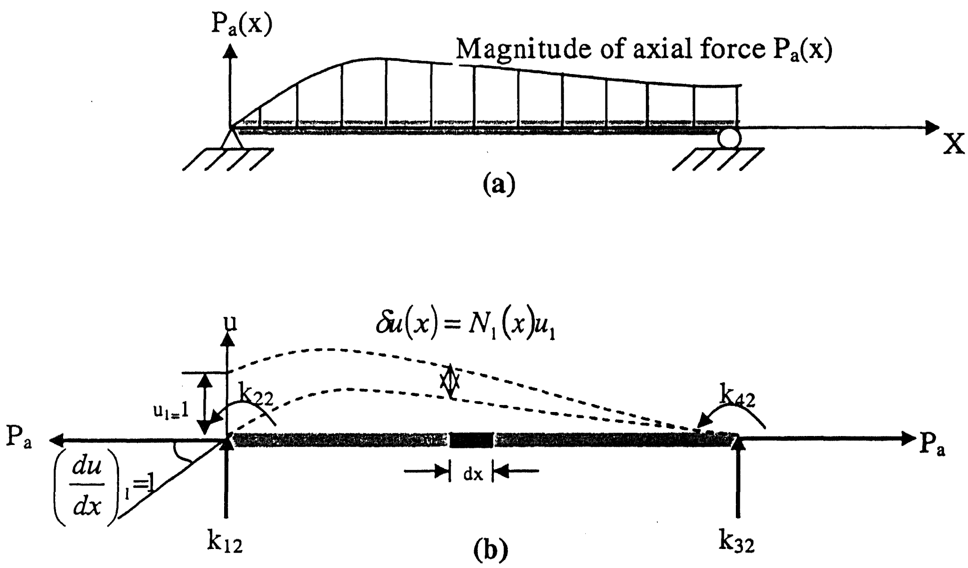


**Fig. 3.5: (a) variation of axial force (b) axially loaded beam with real rotation and virtual translation of node (taken from Clough and Penzien (1993))**

By definition, the nodal forces due to this displacement are the corresponding geometric stiffness coefficients, for example $k_{G12}$ is the vertical force at left end. If now, this left end is subjected to a unit displacement $u_1^e=1$, the resulting external work is

$$W_e=k_{G12}u_1^e \tag{3.12}$$

$$W_e=k_{G12}$$

Since $u_1^e=1$

The internal work done during this virtual displacement is found by considering a differential element of length *dx* from the beam in Fig. 3.5 (b) and shown in enlarged form as in Fig. 3.6.

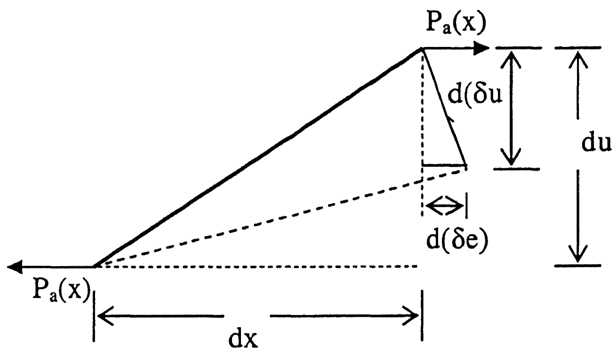


**Fig. 3.6: Enlarged elemental length dx of beam.**

By similar triangles, it may be seen from Fig.3.6.

$$\frac{d(\delta e)}{d(\delta u)}=\frac{du}{dx} \tag{3.13}$$

$$d(\delta e)=\frac{du}{dx}d(\delta u)$$

$$d(\delta e)=\frac{du}{dx}\delta(du)$$

$$d(\delta e)=\frac{du}{dx}\delta\left(\frac{du}{dx}dx\right) \tag{3.14}$$

The work done by the axial force *Pa(x)* during virtual displacement is

$$dW_I = P_a(x)\delta_e \tag{3.15}$$

Where $\delta_e$ represents the relative displacement experienced by the normal force $P_a(x)$ acting on the differential element during virtual displacement.

$$dW_i = P(x)\frac{du}{dx}\delta\left(\frac{du}{dx}\right)dx \tag{3.16}$$

The displacements are expressed in terms of shape functions and integrating finally gives

$$W_i = \int_0^{l_e} P_a(x)\frac{dN_2(x)}{dx}\delta u_1\frac{dN_1(x)}{dx}dx \tag{3.17}$$

$$W_i = \delta u_1\int_0^{l_e} P_a(x)\frac{dN_2(x)}{dx}\frac{dN_1(x)}{dx}dx \tag{3.18}$$

Comparing internal work done with external work done this geometric coefficient is found to be

$$k_{G12} = \int_0^{l_e} P_a(x)\frac{dN_2(x)}{dx}\frac{dN_1(x)}{dx}dx \tag{3.19}$$

Or in general

$$k_{Gij} = \int_0^{l_e} P_a(x)\frac{dN_i(x)}{dx}\frac{dN_j(x)}{dx}dx \tag{3.20}$$

For computer application, above integral is converted to natural coordinate then numerical integration is carried through Gauss quaderature numerical integration scheme.

In natural coordinate system above integral equation (2.24) is

$$k_{Gij} = \frac{2}{l_e}\int_{-1}^{1} P_a(\xi)\frac{dN_i(\xi)}{d\xi}\frac{dN_j(\xi)}{d\xi}d\xi \tag{3.21}$$

Numerical integration is carried through gauss quadrature as

$$[k_G]^e = \sum_{m=1}^{n_g} w_m \left( \frac{2P_a(\xi)}{l_e} \{B\}^e \{B\}^{eT} \right)_{\xi=\xi_m} \tag{3.22}$$

where

$n_g$ is the number of gauss points.

$W_m$ are corresponding weights

Derivative vector $\{B\}^e = \dfrac{d\{N\}^e}{d\xi}$ (3.23)

$\{B\}^{eT}$ is the transpose of $\{B\}^e$. Geometric stiffness matrix is added to beam elemental stiffness matrix to consider the effect of friction and prestress.

## 3.6 Formulation for load vector

The distributed load on foundation beam or the surcharge load on reinforcing beam is considered as distributed load over the beam element as shown in Fig. 3.7 and is converted to nodal forces and moments with the help of Hermitian shape functions $\{N\}^e$ as shown below.

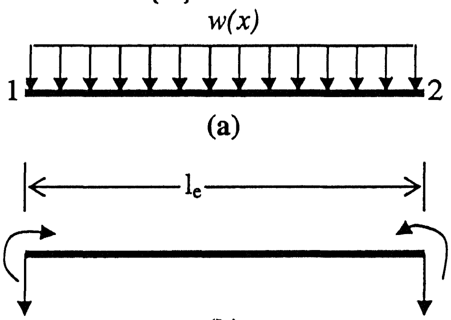


**Fig. 3.7: (a) A typical beam element loaded with UDL and (b) their equivalent loads and moments (taken from Paz (1987))**

The elemental load vector for beam element with distributed load is given by

$$\{f\}^e = \frac{l_e}{2} \int_0^{l_e} w(x) \{N\} dx \tag{3.24}$$

In natural coordinate above equation becomes

$$\{f\}^e = \frac{l_e}{2}\int_{-1}^{1} w(\xi)\{N\}d\xi \tag{3.25}$$

Above equation is numerically integrated by Gauss quaterature numerical integration scheme. Global load vector $\{F\}$ is obtained by assembling the elemental load vectors for foundation beams and reinforcing beams then adding the concentrated load vector $\{F^*\}$ to the assembled load vector (given in the section 3.8.2).

$\{F^*\}$ is given by

$$\{F^*\} = \begin{Bmatrix} W_{2i-1} \\ M_{2i} \end{Bmatrix} \tag{3.26}$$

where

$W_{2i-1}$ are the concentrated forces.

$M_{2i}$ are the concentrated moments.

$i$ = 1,2,3...are global node number at which concentrated load acts.

## 3.7 Mesh details and connectivity of various components

In this section finite mesh details i.e. global node numbering and element numbering for beams (representing foundation beam and reinforcing beam), springs in strong soil and for bottom spring representing poor soil are presented, basic concepts are referred from Cook (1981). Then connectivity matrices are formed for each component i.e. beam elements and spring elements and are used in assemblage of components. Finite element mesh details used to form connectivity matrices is shown in Fig. 3.8.

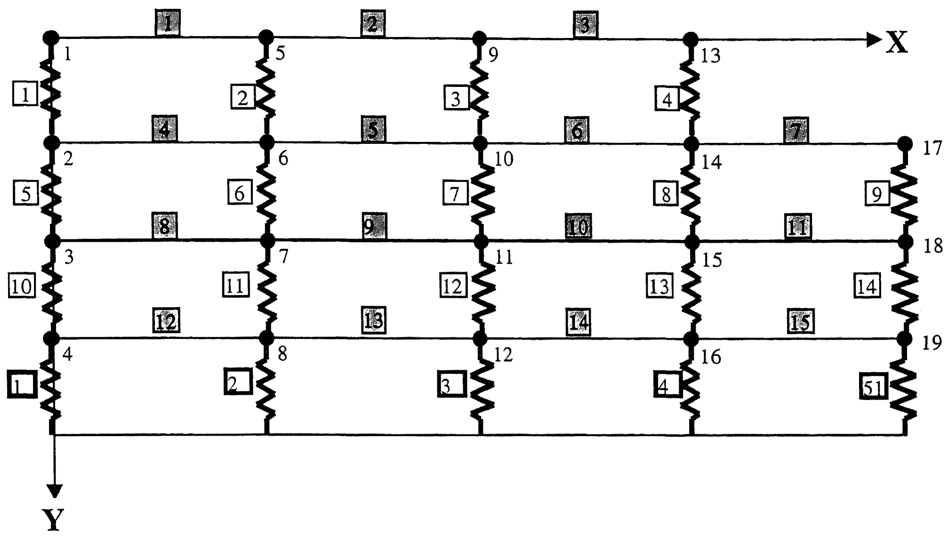


**Fig. 3.8: Finite element mesh details**

1, 2, 3 ... are Global node numbers.

$\boxed{1}$ $\boxed{2}$ $\boxed{3}$ are top spring element numbers.

$\boxed{1}$ $\boxed{2}$ $\boxed{3}$ are beam element numbers.

$\boxed{1}$ $\boxed{2}$ $\boxed{3}$ bottom spring element numbers.

Connectivity matrices for various components are given as:

$$\text{Beam connectivity matrix } \left[C^{b}\right] = \begin{bmatrix} 1 & 5 \\ 5 & 9 \\ 9 & 13 \\ 2 & 6 \\ \vdots & \vdots \end{bmatrix}$$

$$\text{Top springs connectivity matrix } \left[Ck^{t}\right] = \begin{bmatrix} 1 & 2 \\ 5 & 6 \\ 9 & 10 \\ 13 & 14 \\ \vdots & \vdots \end{bmatrix}$$

$$\text{Bottom spring connectivity matrix } \left[Ck^{b}\right] = \begin{bmatrix} 4 \\ 8 \\ 12 \\ 16 \\ \vdots \end{bmatrix}$$

## 3.8 Assembly of elemental matrices

After getting the elemental stiffness matrices, elemental load vector for distributed load and concentrated load vector, it is required to assemble all the elemental stiffness matrices and the load vectors in order to get the final FEM equation. This section focuses on the assembling of various elemental matrices.

### 3.8.1 Assembly of elemental stiffness matrices

Elemental Beam stiffness matrix and elemental spring stiffness matrix are first expanded to the size of global stiffness matrix of size $2n\times 2n$ ($n$ is the total number of global nodes) using simplified assembly relations given below.

$$\left.\begin{aligned}
[K_{2r-1,2s-1}]^e &= [k_{2p-1,2q-1}]^e \\
[K_{2r-1,2s}]^e &= [k_{2p-1,2q}]^e \\
[K_{2r,2s-1}]^e &= [k_{2p,2q-1}]^e \\
[K_{2r,2s}]^e &= [k_{2p,2q}]^e
\end{aligned}\right| \quad \text{when } r = C_{ep} \text{ and } s = C_{eq} \tag{3.27}$$

$$= 0 \qquad \text{otherwise}$$

where,

$[K]^e$ represents expanded elemental matrix elements for beam and spring elements.

$[k]^e$ represents unexpanded elemental matrix elements for beam and spring elements.

$C_{ep}$, $C_{eq}$ are connectivity coefficients of corresponding connectivity matrix.

$p$, $q$ are corresponding local node numbers to beam and spring elements.

$r$, $s$ are corresponding position in global stiffness matrix.

$e$ represent the element considered.

Global stiffness matrix is obtained by adding all the elemental stiffness matrices as in equation (3.28).

$$[K]=\sum_{e=1}^{n_e^f}[K_f]^e+\sum_{e=1}^{n_e^r}[K_r]^e+\sum_{e=1}^{n_e^{k1}}[Kk_t]^e\times nl+\sum_{e=1}^{n_e^{k2}}[Kk_b]^e \tag{3.28}$$

where,

$[K]$ is the global stiffness matrix.

$[K_f]^e$ is expanded elemental stiffness matrix of foundation beam

$[K_r]^e$ is expanded elemental stiffness matrix of reinforced beam

$[Kk_t]^e$ is expanded elemental stiffness matrix of top soil sub grade modulus

$[Kk_b]^e$ is expanded elemental stiffness matrix of lower soil sub grade modulus.

$n_e^f$ is number of elements of foundation beam.

$n_e^r$ is number of elements of reinforcement beams.

$n_e^{k_1}$ is number of elements of springs representing compact dense soil.

$n_e^{k_2}$ is number of elements of springs representing poor soil.

$nl$ is the number of layers of reinforcements.

### 3.8.2 Assembly of elemental load vectors

Elemental load vectors are first expanded to the size of global load vector of size $2n$ using simplified assembly relations as given below.

$$\left.\begin{aligned}\{F_{2r-1}\}^e &= \{f_{2p-1}\}^e \\ \{F_{2r}\}^e &= \{f_{2p}\}^e\end{aligned}\right|\quad \text{when } r = C_{ep} \tag{3.29}$$

$$= 0 \qquad \text{otherwise}$$

where,

$\{F\}^e$ represents expanded load vector elements for beam elements.

$\{f\}^e$ represents elemental unexpanded load vector for beam elements.

$C_{ep}$, are connectivity coefficients of corresponding connectivity matrix.

$p$ is corresponding local node numbers to beam and spring elements.

$r$ is the position of element in global matrix.

$e$ represent the element considered.

Global load vector is found by adding all the elemental load vectors and the concentrated load vector as shown below.

$$\{F\} = \sum_{e=1}^{n_e^f} \{F_f\}^e + \sum_{e=1}^{n_e^r} \{F_r\}^e + \{F^*\} \tag{3.30}$$

where,

$\{F\}$ is the global load vector.

$\{F_f\}^e$ is expanded elemental load vector of foundation beam.

$\{F_r\}^e$ is expanded elemental load vector of reinforcement beam.

$\{F^*\}$ is the concentrated load vector.

$n_e^f$ is number of elements of foundation beam.

$n_e^r$ is number of elements of reinforcing beams.

## 3.1 Final FEM equation

FEM equation in matrix form is given by

$$[K]\{u\} = \{F\} \tag{3.31}$$

where

$[K]$ is the global stiffness matrix.

$\{u\}$ is the global displacement vector and is given by
$$\{u\} = \begin{Bmatrix} u_1 \\ \left(\dfrac{du}{dx}\right)_1 \\ \cdot \\ \cdot \\ u_n \\ \left(\dfrac{du}{dx}\right)_n \end{Bmatrix} \tag{3.32}$$

where

$u_i$, are the displacements of beam at global node i=1,2,3...$n$.

$\left(\dfrac{du}{dx}\right)_i$ are the rotations of beam at global node i=1,2,3...$n$.

$n$ is the total number of global node.

## 3.10 Application of boundary condition

Since the geometry and loading of the model considered is symmetrical, the rotation of foundation and reinforcing beams at the centre is zero corresponding elements in global load vector is made zero and corresponding elements in global stiffness matrix are made 1.

## 3.11 Solving the FEM equation

After applying boundary conditions the FEM equation is solved by gauss elimination method.

Above formulations and analysis described in this chapter are used to analyze the problem considered in the present study and results from the analysis are discussed in chapter 4.

# CHAPTER 4

# RESULTS AND DISCUSSIONS

## 4.1 General

Following the statement of the problem and problem formulation by FEM as described in chapter 3, a computer program in language C is developed. The validity of the program and the convergence of the solution are checked first and then detailed results for parametric study are obtained. All the computations have been carried out on a personal computer with 2400+ AMD processor and 256 MB RAM. Since the problem considered is symmetrical with respect to geometry as well as in loading condition, only half portion of the system is studied and presented.

## 4.2 Convergence study and Validation of the model

The problem consists of foundation beam and the reinforcing beam having equal length with one layer of reinforcement subjected a concentrated load acting at the center is solved for three discretizations of 40, 80, 160 beam elements (for each foundation beam and reinforcing beam). The parameters used are $l_l$=16m, $z_r = 1$, $R = 10$, $r = 5$, $R_l = 1$, $k_1 = 50$ MN/m$^3$, $\gamma' = 0$ and $Q = 100000$ N. For all three discretizations the normalized deflections at the centre and at the edge of foundation beam as well as reinforcing beam are tabulated in table 4.1. It is observed that the values of normalized deflection at centre and at edge almost converge for 160 elements.

**Table 4.1: Values of deflection for three discretizations**

| Discretization | Normalized deflection at the centre | | Normalized deflection at the edge | |
|---|---|---|---|---|
| | Foundation beam ($y_1'$) | Reinforcing beam ($y_2'$) | Foundation beam ($y_1'$) | Reinforcing beam ($y_2'$) |
| 40 elements | 1.22551 | 0.0999994 | $2.30476\times10^{-3}$ | $1.94588\times10^{-4}$ |
| 80 elements | 1.27784 | 0.104006 | $2.60460\times10^{-3}$ | $2.19902\times10^{-4}$ |
| 160 elements | 1.30571 | 0.106116 | $2.77631\times10^{-3}$ | $2.34401\times10^{-4}$ |

The present FEM model results are validated by comparing it with the closed form solution obtained by Maheshawari (2004) for both foundation beam and the reinforcing beam having equal length with one layer of reinforcement subjected to concentrated load acting at the center. While validating the program three hundred beam elements are taken for each foundation and reinforcing beam. The results from the present study for typical values of parameters are found to be in exact agreement with the results obtained by Maheshwari (2004) as shown in Fig 4.1. While validating the model results, the deflections of reinforcing beam are normalized as $y_2' = \dfrac{y_2 E_2 I_2}{Q_t R_2^3}$ (same as Maheshwari (2004)).

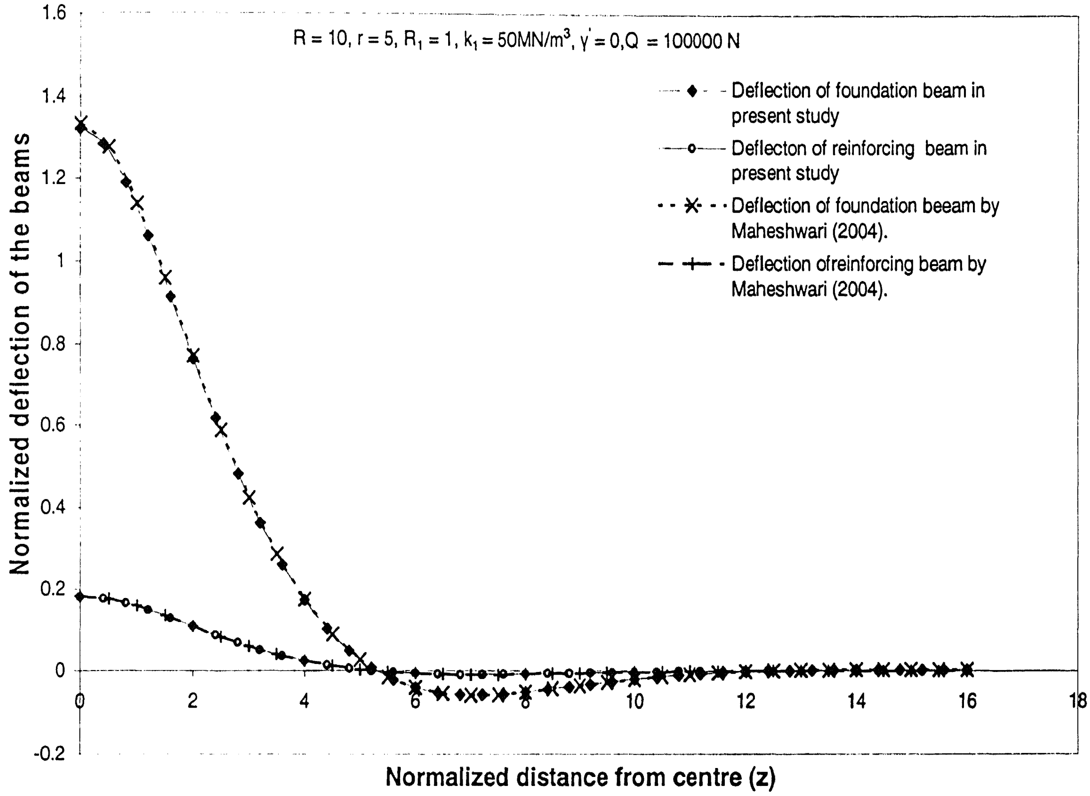


**Fig. 4.1: Comparison of deflection profile of beams with Maheshwari (2004)**

## 4.3 Parametric study

The model after validation for one layer of reinforcement has been used to study the effect of multilayer reinforcement. The effects of various parameters and the effect of number of layers of reinforcement on settlement response of foundation beam and reinforcing beams are presented in the following sections. Maheshwari (2004) concluded that there is no significant influence on deflection of foundation beam when $z_r$ is more than 1.5 for one layer of reinforcement and the same was observed for multilayer reinforcement hence in this present study for all parametric values the ratio of non-dimensional length of reinforcing beam to non-dimensional length of foundation beam is kept 1.5. The foundation beam is assumed to be smooth and no prestress forces are considered.

### 4.3.1 Ranges of the non dimensional parameters

The ranges of the non-dimensional parameters used in the present study are tabulated in Table 4.2.

**Table 4.2: The ranges of non-dimensional parameters**

| Non-dimensional parameters | Ranges |
|---|---|
| Non-dimensional depth of placement h' | 0.5 -1.5 |
| Relative flexural rigidity of foundation beam and reinforcing beam, $R = \frac{E_1 I_1}{E_2 I_2}$ | 10 - 60 |
| Relative stiffness of the soil layers, $r = \frac{k_1}{k_2}$ | 1 - 20 |
| Non-dimensional unit weight of upper layer of soil, $\gamma' = \frac{\gamma R_1^2}{Q_t}$ | 0.05 - 1 |

### 4.3.2 The effect of number of layers of reinforcement on Settlement response of foundation beam

Following cases have been investigated for the study of effect of number of layer of reinforcement.

a. Unreinforced case: This has been simulated using negligible bending stiffness of reinforcing beam i.e. $E_2 I_2$ is of the order $10^{-10}$.

b. Single layer of reinforcement.

c. Two layer of reinforcement.

d. Three layer of reinforcement.

e. Four layer of reinforcement.

f. Five layer of reinforcement

All the above cases have been shown in Fig. 4.2 and Fig 4.3 for concentrated load at the centre of foundation beam and concentrated loads at the edges of foundation beam respectively. It is observed that increasing number of reinforcing layer beyond three does not have significant influence on the deflection profile of the foundation beam. The percentage reduction in the maximum normalized deflection of the foundation beam due to inclusion of various numbers of reinforcing layers with respect to unreinforced earth has been given in table 4.3 for load acting at centre and at edges respectively.

**Table 4.3: Effect of number of layers of reinforcements on maximum deflection of foundation beam**

| Case | Percentage reduction in maximum settlement with respect to unreinforced soil | |
|---|---|---|
| | Concentrated load at centre | Concentrated load at edges |
| Single layer | 18.15 | 22.76 |
| Two layer | 21.80 | 30.34 |
| Three layer | 23.26 | 34.83 |
| Four layer | 24.04 | 37.93 |
| Five layer | 24.54 | 40.00 |

From Fig. 4.2 it is observed that for concentrated load at the centre of foundation beam, effect of number of layers of reinforcement on maximum normalized deflection i.e. at the centre of foundation beam is significant and the reduction in maximum normalized deflection is up to 23 % with respect to unreinforced earth when three layers of reinforcements are considered. It is found that

when one layer of reinforcement is used the percentage reduction in maximum normalized is maximum and is 18 % among all layers of reinforcement. The reduction in settlement due to adding second and third layer is 3-4 and 1-2 % respectively. Further adding reinforcement has negligible effect on deflection profile of foundation beam.

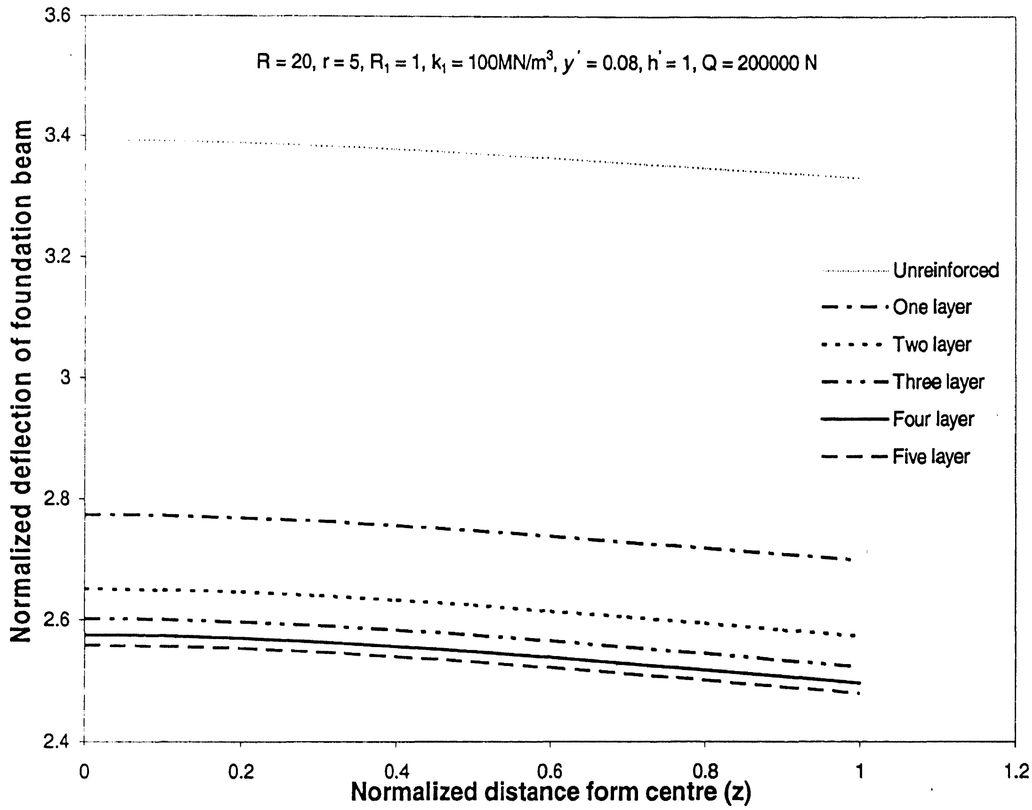


**Fig. 4.2: Effect of number of layers of reinforcement on deflection profile of foundation beam subjected to concentrated force at its centre**

From Fig. 4.3 it is observed that the for concentrated load at edges of foundation beam, effect of number of layers of reinforcement on maximum normalized deflection i.e. at the edges of foundation beam is significant and the reduction in maximum normalized deflection is up to 35 % with respect to unreinforced earth when three layers of reinforcements are considered. This reduction is more than that of the case when load is acting at centre. The reason is that in case of

load acting at edges foundation beam offers less resistance compared to the case when load is at the centre. Subsequently the reinforcing beam offers more resistance. It is found that when one layer of reinforcement is used the percentage reduction in maximum normalized deflection is maximum and is 23 % among all layers of reinforcement. The reduction in settlement due to adding second and third layer is 7% and 5 % respectively. Further, adding more reinforcement has negligible effect on deflection profile of foundation beam.

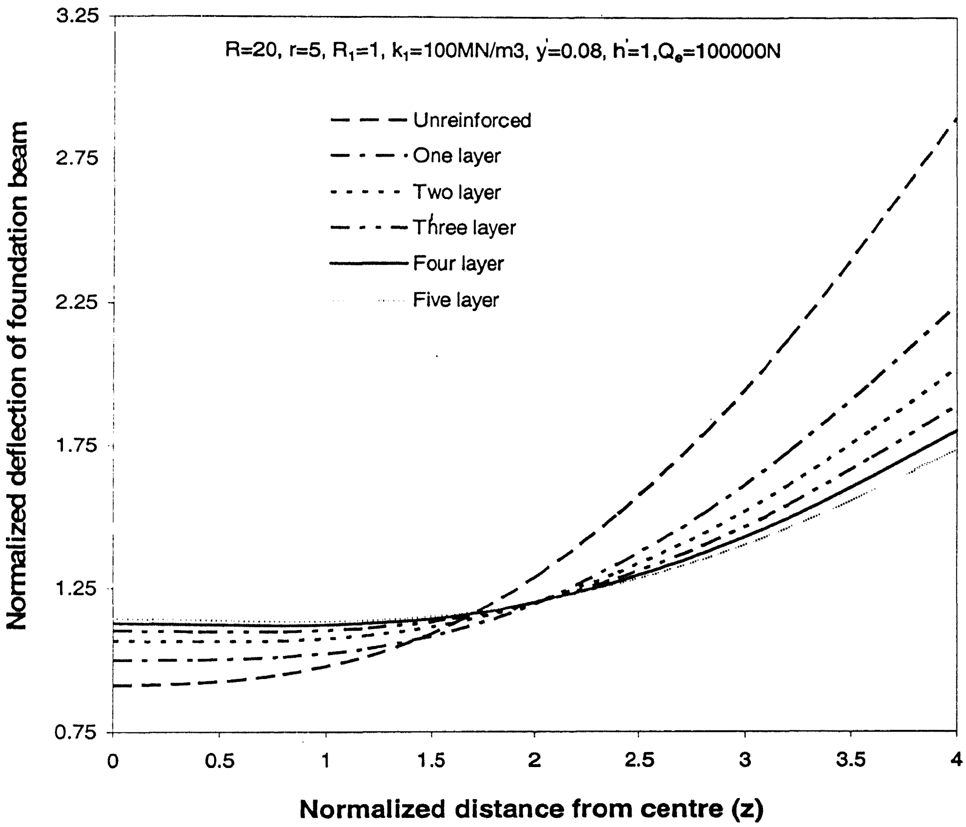


**Fig. 4.3: Effect of number of layers of reinforcement on deflection profile of foundation beam subjected to concentrated force at its edges**

As it has been observed that increasing the number of layer of reinforcements beyond three does not have significant influence on the deflection profile of foundation beam, in the following sections for all the parametric studies only three layers of reinforcement are considered. For the study on deflection profile of

reinforcing beams, the deflection profile for layer - 1 (the layer nearer to the foundation beam) and layer - 3 (the layer at the soil interface) are shown. The deflection profile for the middle reinforcing layer is not shown, and its deflection profile lies in between that of layer - 1 and layer - 3.

### 4.3.3 *Effect of load*

The effect of load $Q_t$ is studied through varying non-dimensional parameter $\gamma^{'}(=\frac{\gamma R_1^2}{Q_t})$ and keeping related parameters other than $Q_t$ constant. The parameter $\gamma^{'}$ decreases with increase in load $Q_t$. Since $R_1$ depends on parameters such as stiffness of foundation beam and coefficient of subgrade reaction of upper layer of soil layer, these are fixed as $R = 20$, $r = 5$, $h'=1$, $z_r = 1.5$, $R_1 = 1$ and the same is used for further parametric studies in the following sections.

In Fig 4.4 and Fig. 4.5, the deflection profiles for the foundation and the reinforcing beams are presented respectively for a set of typical values of parameters, showing the effect of a concentrated load at the center of the foundation beam through variation of $\gamma^{'}$. Fig. 4.6 and Fig. 4.7 shows similar plots for the foundation beam subjected to end loads. The load parameter $Q_t$ appears in the non-dimensional deflection parameters $y_1^{'} = \frac{y_1 E_1 I_1}{Q_t R_1^3}$ and $y_2^{'} = \frac{y_1 E_1 I_1}{Q_t R_1^3}$ in the denominator. Therefore, for lower loads higher non-dimensional deflections are observed which actually imply lower deflections in dimensional form.

From Fig. 4.4 it observed that the maximum normalized deflection occurs at the centre and decreases to minimum towards the edge. The maximum normalized deflection at the centre decreases by 75 % and minimum normalized deflection at edge decreases from 0.253 to 5.32 as $\gamma^{'}$ decreases from 1 to 0.05.

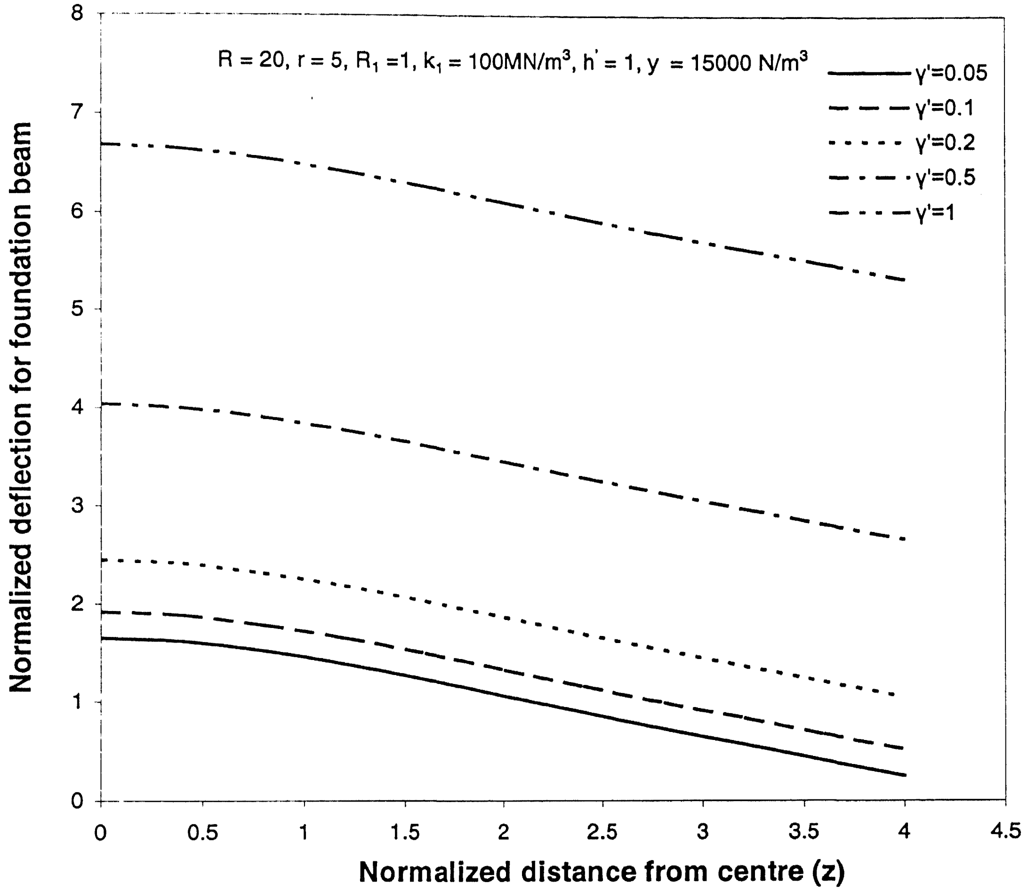


**Fig. 4.4: Normalized deflection of foundation beam for various values of $\gamma'$ for load acting at the centre**

From Fig. 4.5 it is observed that the maximum normalized deflection occurs at the centre and decreases to minimum and becomes constant towards the edges. The maximum normalized deflections of layer – 1 and layer – 3 decrease by 76 % and 77% respectively as $\gamma'$ decreases from 1 to 0.05 and the minimum normalized deflections at the edge of layer – 1 and layer – 3 decrease by 97 % as $\gamma'$ decreases from 1 to 0.05. It is seen that at lower load e.g. $\gamma' = 1$ layer – 1 has more influence than that of layer – 3.

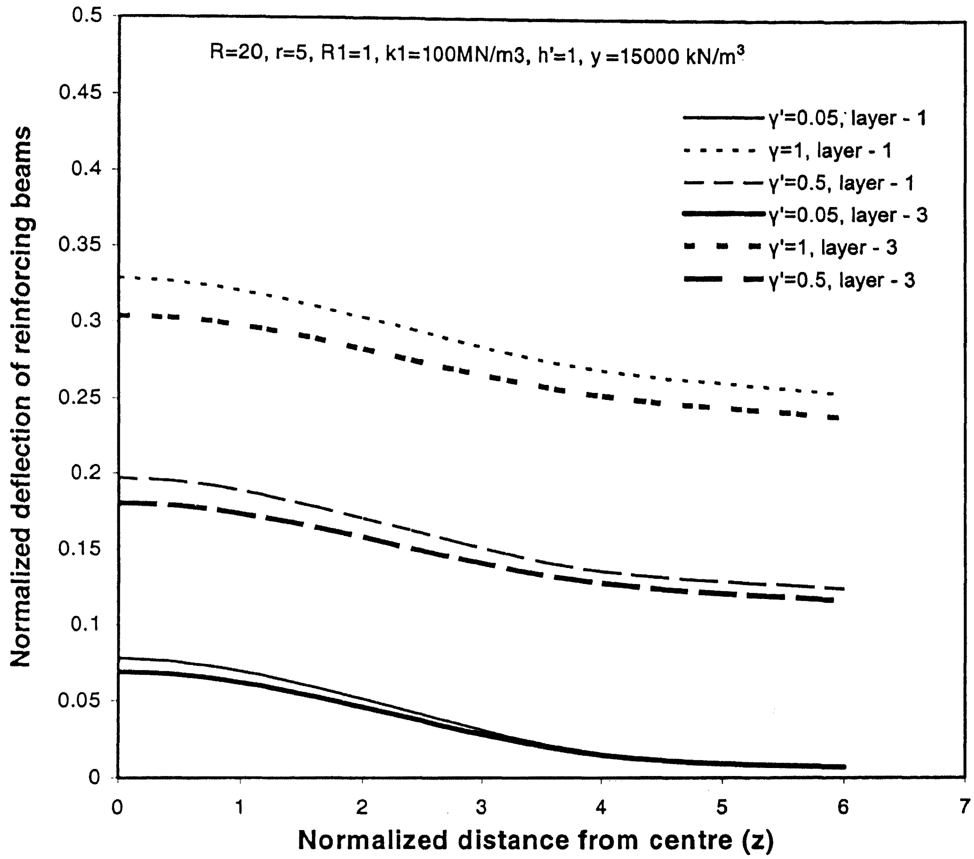


**Fig. 4.5: Normalized deflection of reinforcing beams for various values of $\gamma'$ for load acting at the centre**

From Fig. 4.6 it observed that the maximum normalized deflection occurs at the edges and decreases to minimum towards the centre. The maximum normalized deflection at edge decreases by 75 % and minimum normalized deflection at the centre decreases by 84 % as $\gamma'$ decreases from 1 to 0.05.

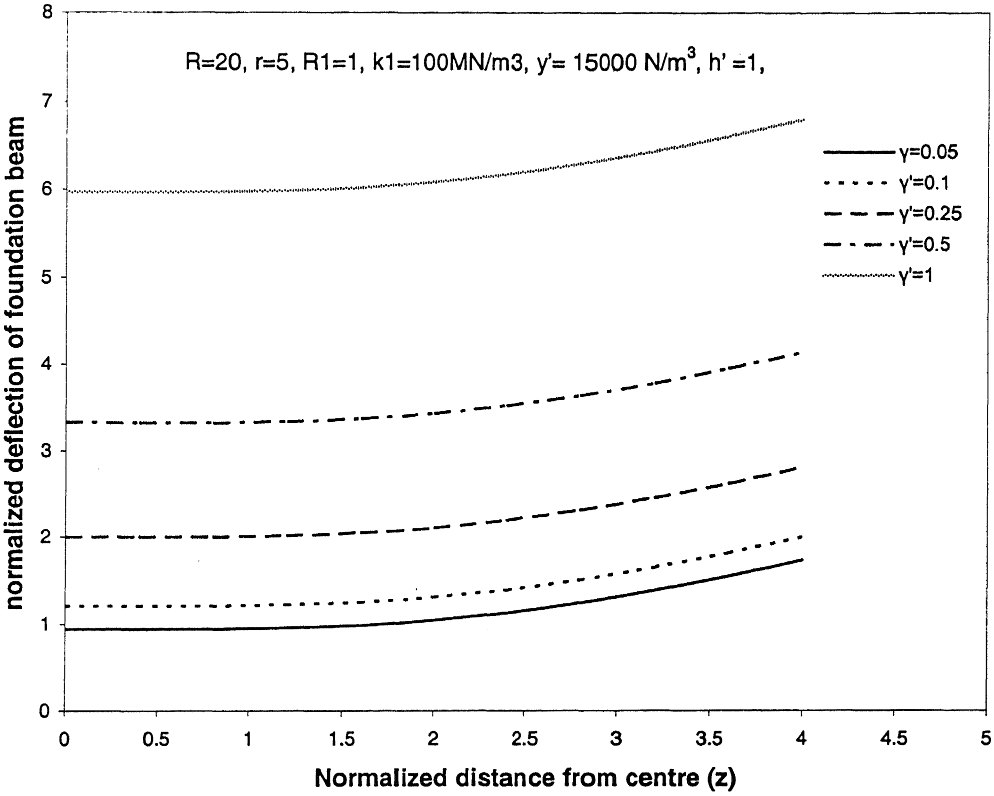


**Fig. 4.6: Normalized deflection of foundation beam for various values of $\gamma'$ for loads acting at the edges**

From Fig. 4.7 it is observed that the maximum normalized deflection occurs at z = 3.6 and decreases to minimum towards the edges. The maximum normalized deflections of layer – 1 and layer – 3 decrease by 78 % and 80 % respectively as $\gamma'$ decreases from 1 to 0.05 and minimum normalized deflections at the edge of layer – 1 and layer – 3 decrease by 97 % as $\gamma'$ decreases from 1 to 0.05. It is seen that at lower load $\gamma'$ = 1 layer – 1 has more influence than that of layer – 3. The normalized deflections at the centre of layer – 1 and layer – 3 decrease by 85 % as $\gamma'$ decreases from 1 to 0.05.

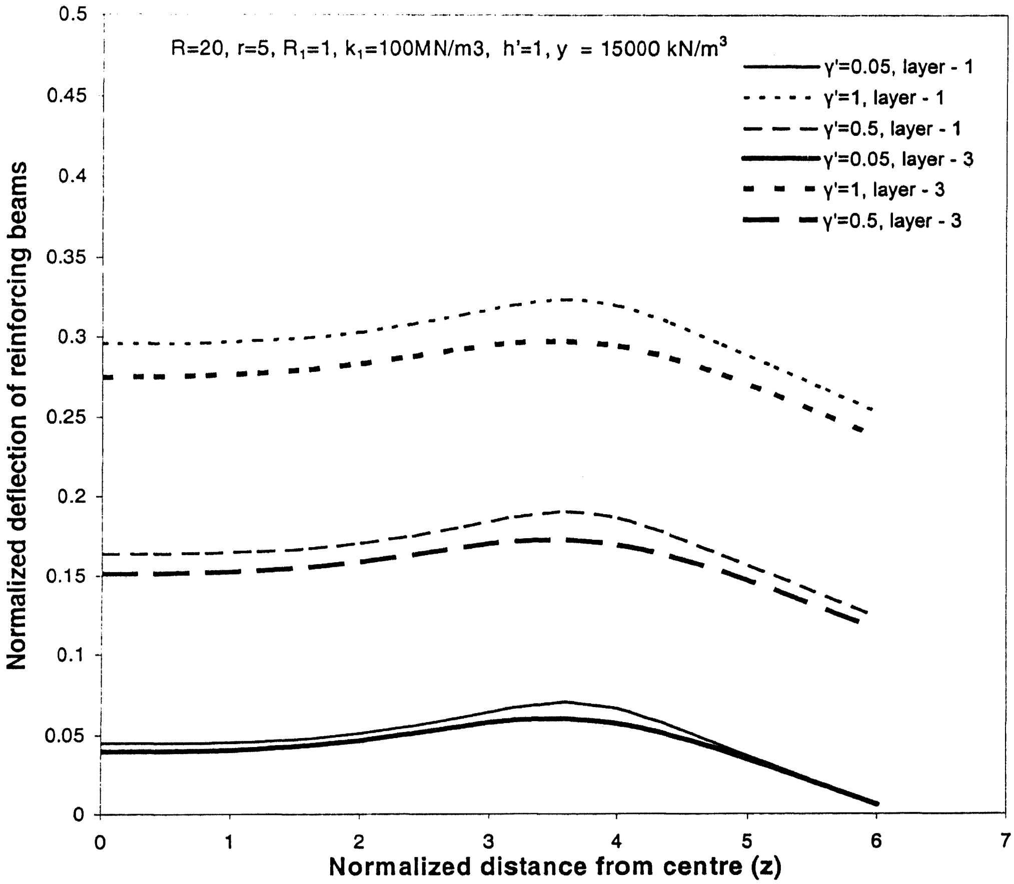


**Fig. 4.7: Normalized deflection of reinforcing beams for various values of $\gamma'$ for loads acting at the edges**

### 4.3.4 Effect of depth of placement of reinforcements

In Fig 4.8 and Fig 4.9, the deflection profiles for the foundation and the reinforcing beams are presented respectively for a set of typical values of parameters, showing the effect of depth of placement of reinforcement for a concentrated load at the center of the foundation beam. Fig. 4.10 and Fig. 4.11 shows similar plots for the foundation beam subjected to end loads.

From Fig. 4.8 it is seen that maximum deflection occurs at the centre of the beam and then decreases gradually to lowest towards the edges of the beam. With the increase in normalized depth of placement from 0.5 to 1.5, the maximum normalized deflection at the centre increases by 26 % while corresponding deflection at the edge

of the beam increases from 0.2 to 0.63. As the depth of placement increases all the reinforcement layers are offering less resistance resulting in increase in deflection.

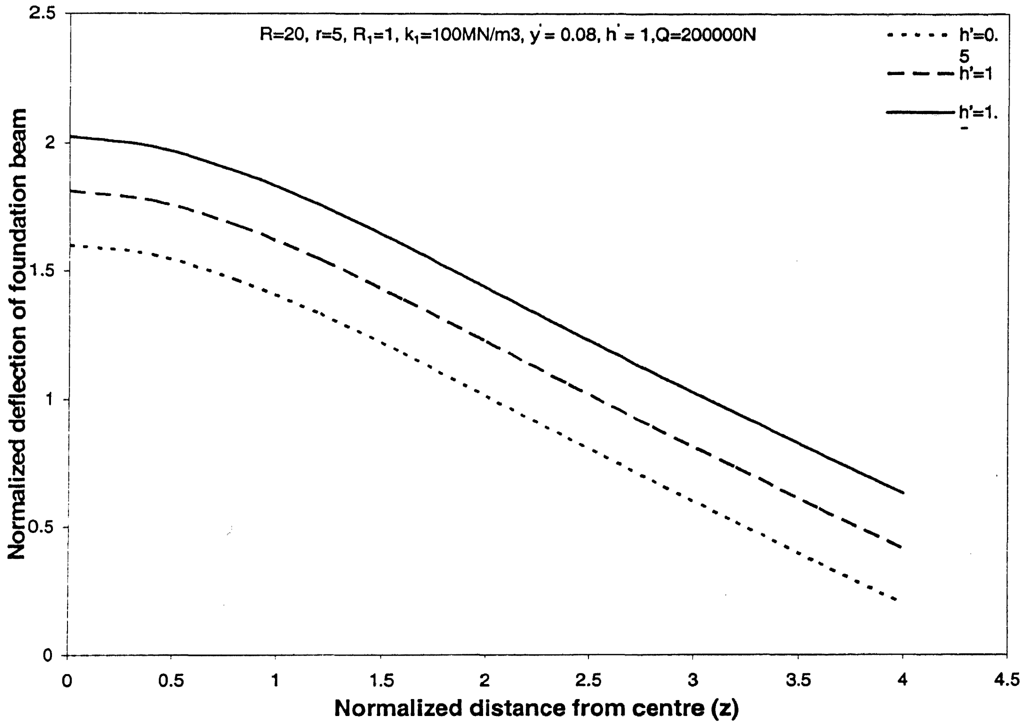


**Fig. 4.8: Normalized deflection of foundation beam for various values of $h'$ for load acting at the centre**

Fig. 4.9, it can be seen that the maximum deflection of reinforcing beams occurs at the centre and decreases to a constant value towards the edge. The layer one deflects more than layer three for same depth of placement at the centre of reinforcement. This shows that reinforcing beam near to the foundation have greater influence. The increase in maximum deflection for layer - 1 and layer - 3 at centre of beam is around 27 % and 30 % respectively as normalized depth of placement increases from 0.5 to 1.5. The minimum normalized deflection at the edge increases by 80 % for both layer -1 and layer – 3 as h' increases from 0.5 to 1.5. Deflection profiles for various normalized deflection become parallel at the edges. This shows that deflections at edges are mainly due to surcharge.

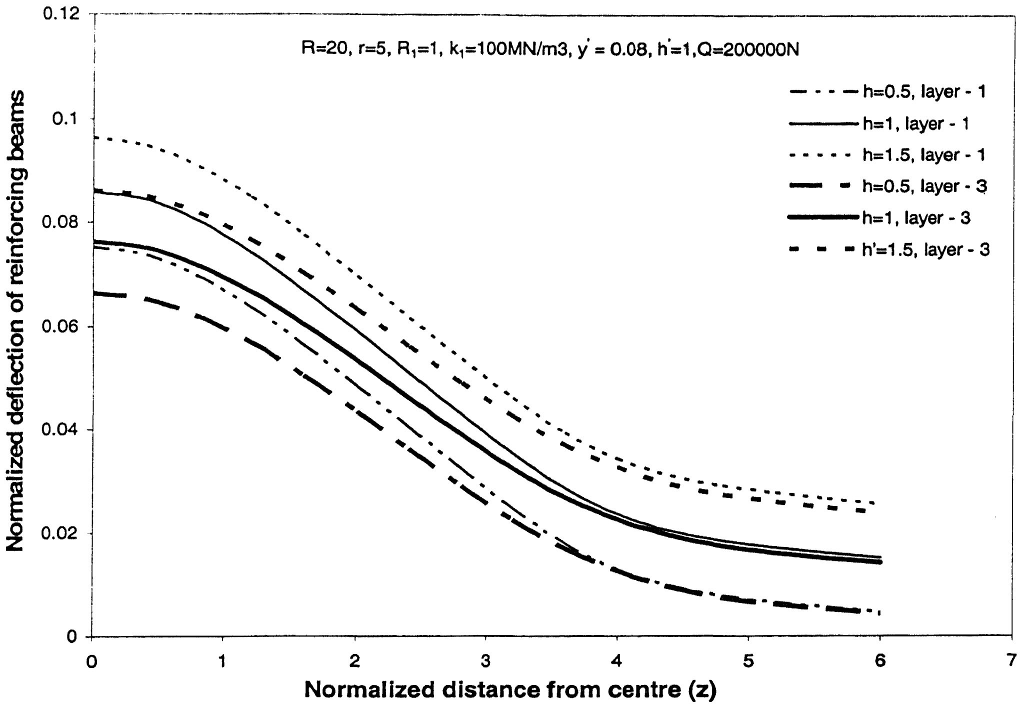


**Fig. 4.9: Normalized deflection of foundation beam for various values of $h'$ for load acting at the centre**

From Fig. 4.10 it is observed that maximum deflection in the foundation beam occurs at the point of application of the load, i.e., at the edge of the beam, then decreases gradually towards the centre of the beam and becomes least at the centre of the beam. It is observed from the figure that as the normalized depth of placement increases from 0.5 to 1.5, the maximum normalized deflection at edge of foundation beam increases by 25 % and normalized deflection at the centre increases by 48 %.

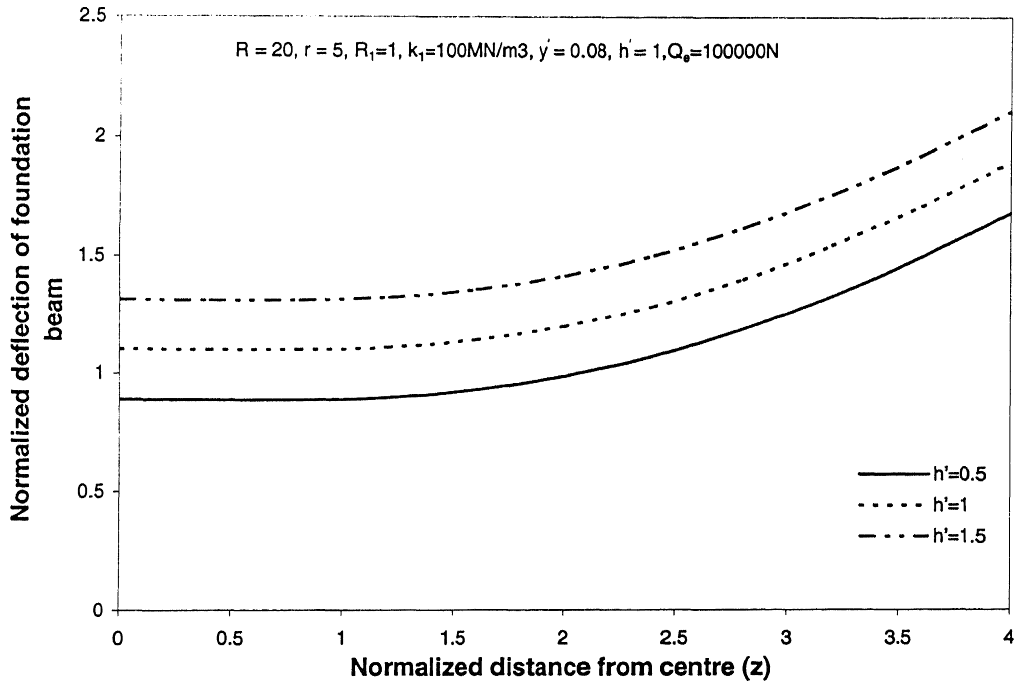


**Fig. 4.10: Normalized deflection of foundation beam for various values of $h'$ for loads acting at the edges**

Fig. 4.11 shows that the maximum deflection occurs at z = 3.6, decreases rapidly towards the edge of beam because of less resistance from foundation beam and gradually decreases towards the centre of beam and becomes constant. The minimum deflection occurs at the edges of reinforcing beams. As normalized depth of placement increases from 0.5 to 1.5 the maximum normalized deflections at z = 3.6 increase by 32 % and 35 % for layer - 1 and layer – 3 respectively. The normalized deflections at the centre increase by 50 % and 53 % for layer – 1 and layer -3 respectively.

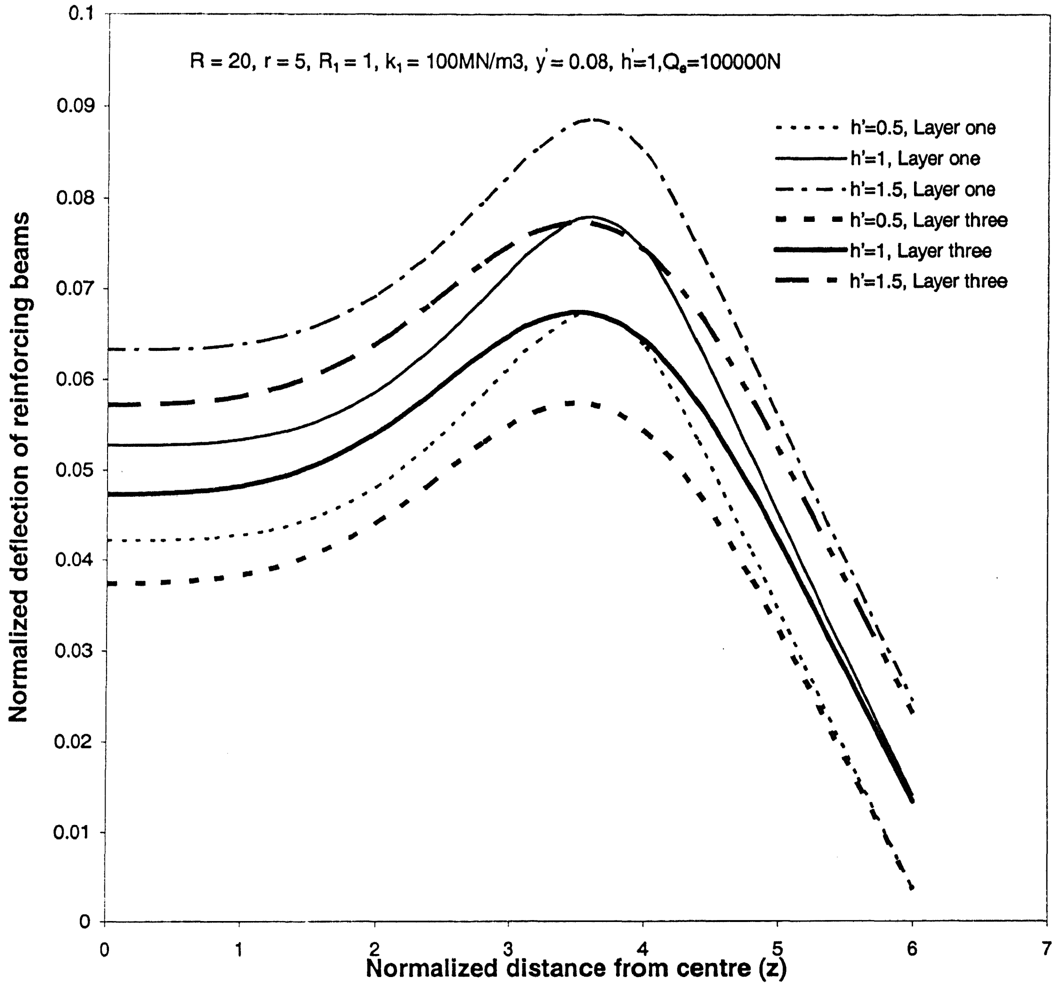


**Fig. 4.11: Normalized deflection of reinforcing beams for various values of $h'$ for loads acting at the edges**

### 4.3.5 Effect relative flexural rigidity of beams

In Fig 4.12 and 4.13, the deflection profiles for the foundation and the reinforcing beams are presented respectively for a set of typical values of parameters, showing the effect of relative flexural rigidity of beams for a concentrated load at the center of the foundation beam. Figs. 4.14 and 4.15 show similar plots for the foundation beam subjected to end loads. The relative flexural rigidity $R$, affects the settlement response of foundation beam and reinforcing beams significantly.

From Fig. 4.12 it is observed that for the foundation beam the maximum deflection occurs at the centre of the beam and gradually decreases to minimum at the edge. The straight portion of the deflection profile towards the edge shows that the deflection at the edge is mainly due to rigidity of the beam. It is observed that with the increase in the ratio $R$ there is an increase in maximum deflection and this increase in deflection becomes negligible after a value of $R$ = 40. As the value of R increases from 10 to 60 the maximum normalized deflection increases by 4 %. For higher values of $R$ ($R$ = 40 and $R$ =6 0) negative deflections at the edges are observed.

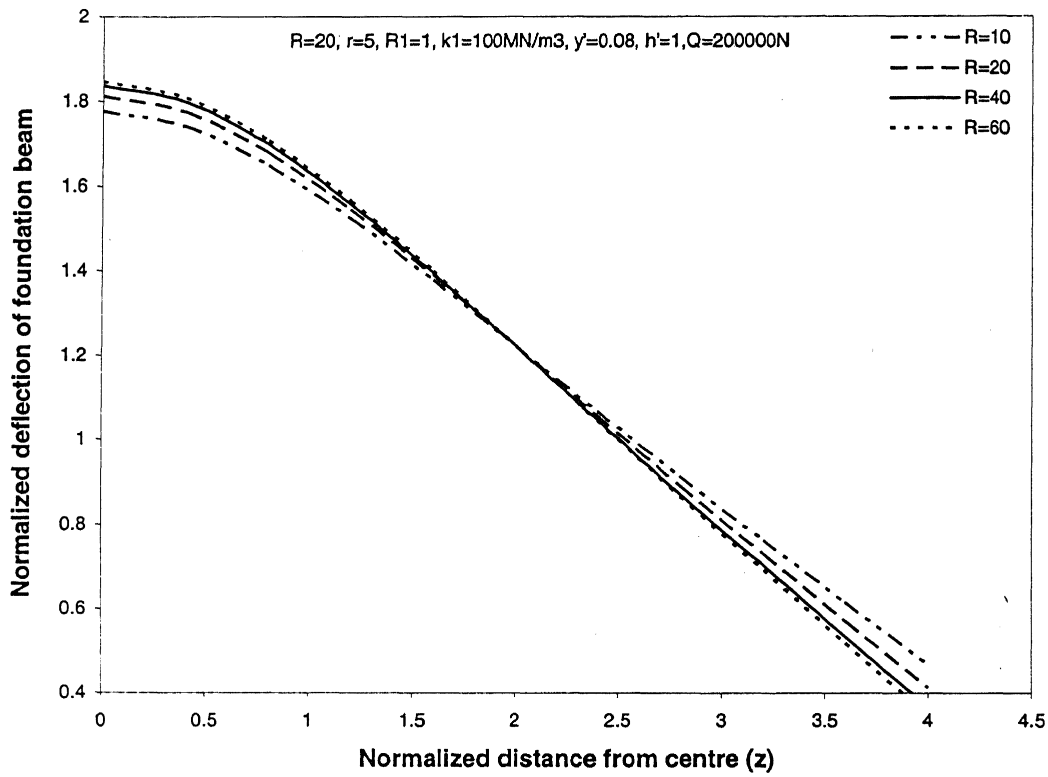


**Fig. 4.12: Normalized deflection of foundation beam for various values of *R* for load acting at the centre**

Fig.4.13 shows that the maximum normalized deflection is observed at the centre of the beams, it gradually decreases towards the edge and finally becomes constant. It is observed that as ratio $R$ increases from 10 to 60 the normalized

deflections decrease by 82 % and 66 % for layer - 1 and layer – 3 respectively. As ratio $R$ increases flexural rigidity of reinforcing beam decreases hence higher deflections are observed. The minimum normalized deflections at the edges decrease by 73 % for both layer – 1 and layer -3.

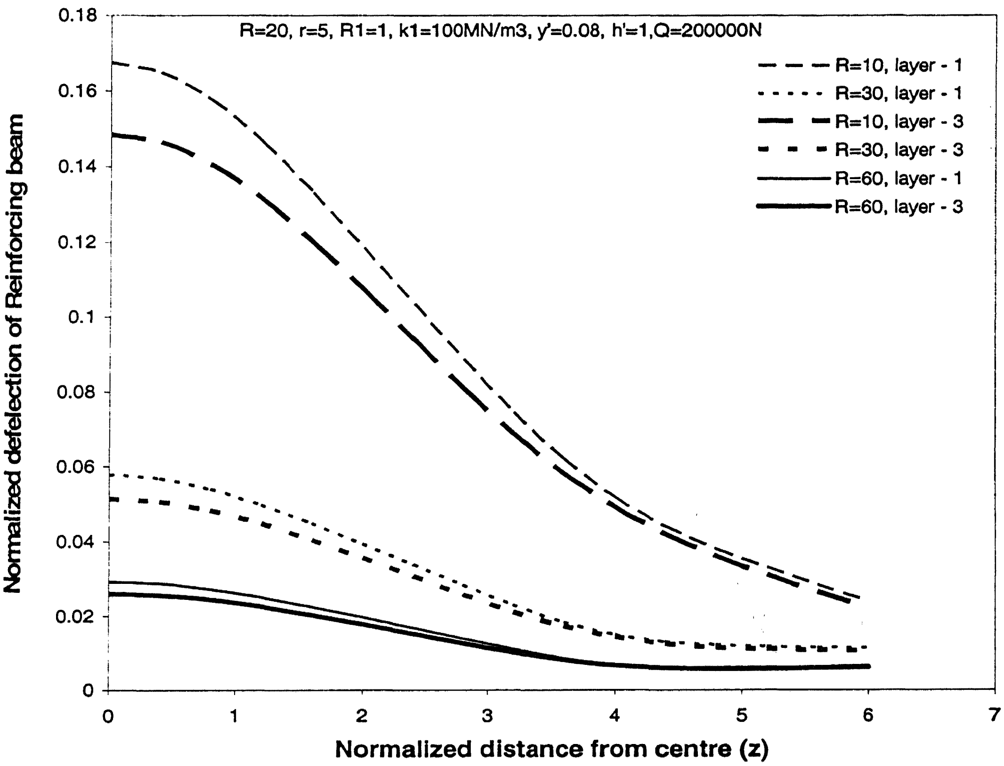


**Fig. 4.13: Normalized deflection of reinforcing beams for various values of *R* for load acting at the centre**

Fig. 4.14 shows that the maximum deflection is observed at the edges of the beam and it increases by 17 % as the ratio $R$ increases from 10 to 60. The minimum deflection is observed at the centre of the beam and it decreases by 7 % as the ratio $R$ increases from 10 to 60.

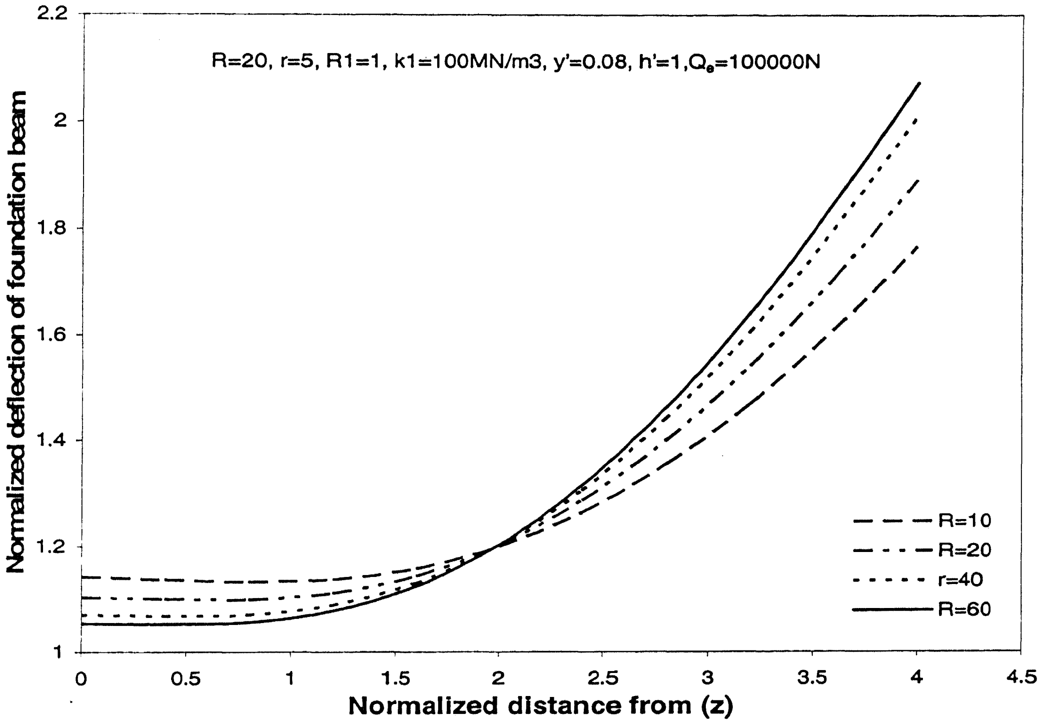


**Fig. 4.14: Normalized deflection of foundation beam for various values of *R* for loads acting at the edges**

From Fig. 4.15, it is seen that the maximum normalized deflection occurs at z = 3.6. It is observed that as the ratio *R* increases from 10 to 60 maximum normalized deflections at z =3.6 decrease by 80 % for both layer - 1 and layer -3. The normalized deflections at the centre decrease by 85 % for both layer – 1 and layer – 3. The minimum normalized deflections the edges decrease by 96 % for both layer – 1 and layer -3.

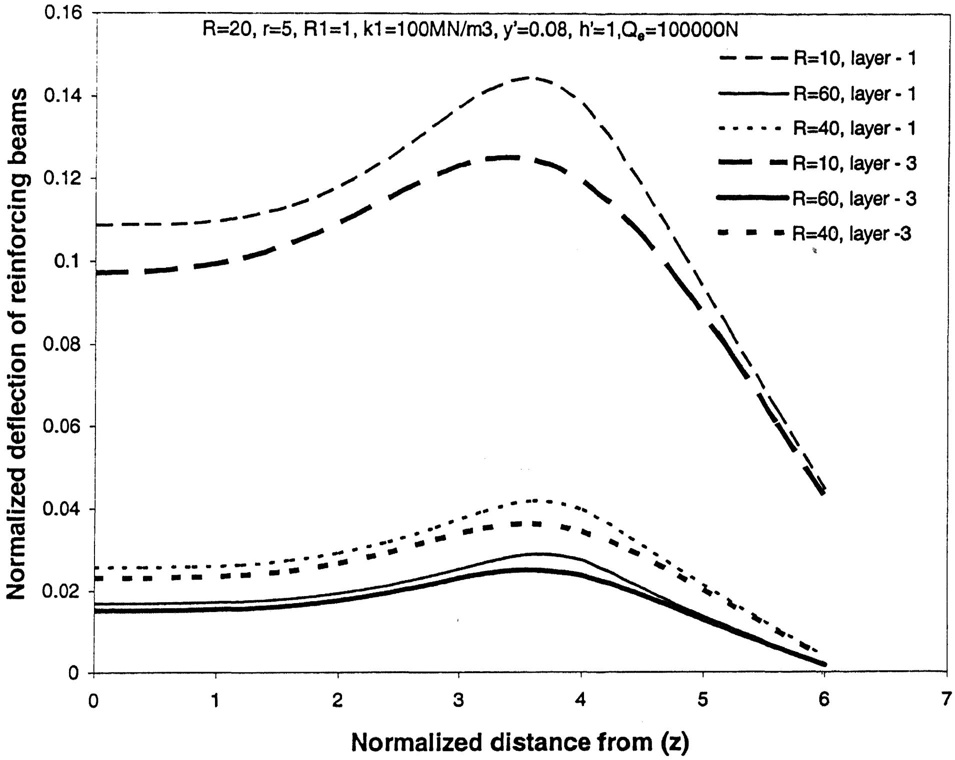


**Fig. 4.15: Normalized deflection of reinforcing beams for various values of *R* for loads acting at the edges**

### 4.3.6 Effect of relative stiffness ratio of the soils

In Fig 4.16 and Fig. 4.17, the deflection profiles for the foundation and the reinforcing beams are presented respectively for a set of typical values of parameters, showing the effect of variation of stiffness ratio of upper layer soil and lower layer soil *r* for a concentrated load at the center of the foundation beam. Figs. 4.18 and Fig. 4.19 show similar plots for the foundation beam subjected to end loads.

From Fig. 4.16 it is observed that for the load acting at the center, the maximum normalized deflection on foundation beam occurs at the centre and increases from 0.7 to 5.24 as the ratio *r* increases from 1 to 20. As the ratio r increases the lower soil becomes poor and hence the increase in deflection is observed. The minimum deflection at edge increases from 0 to 2.57 as *r* increases from 1 to 20.

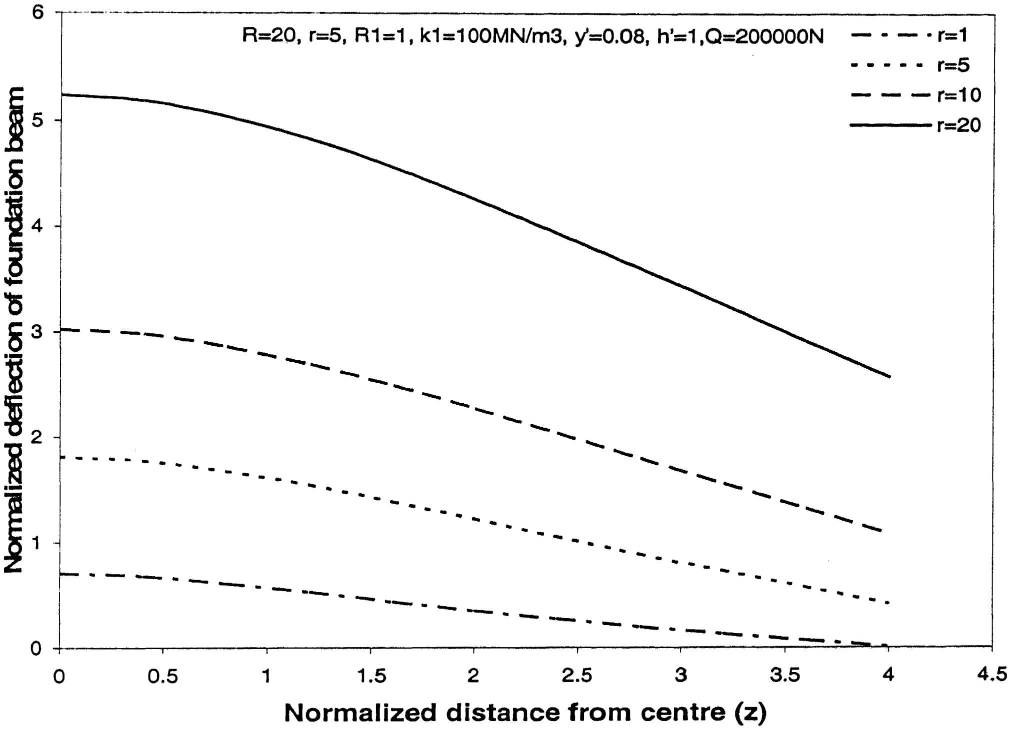


**Fig. 4.16: Normalized deflection of foundation beam for various values of *r* for load acting at the centre**

Fig. 4.17 shows that the maximum normalized deflection, occurs at the centre of the beam, increases from 0.03 to 0.26 and 0.018 to 0.25 for layer -1 and layer - 3 respectively as *r* increases from 1 to 20 and gradually decrease to minimum deflection at the edge of the beam. The normalized deflection at edge increases from 0.004 to 0.023 as *r* increases from 1 to 20 for both layer – 1 and layer -3.

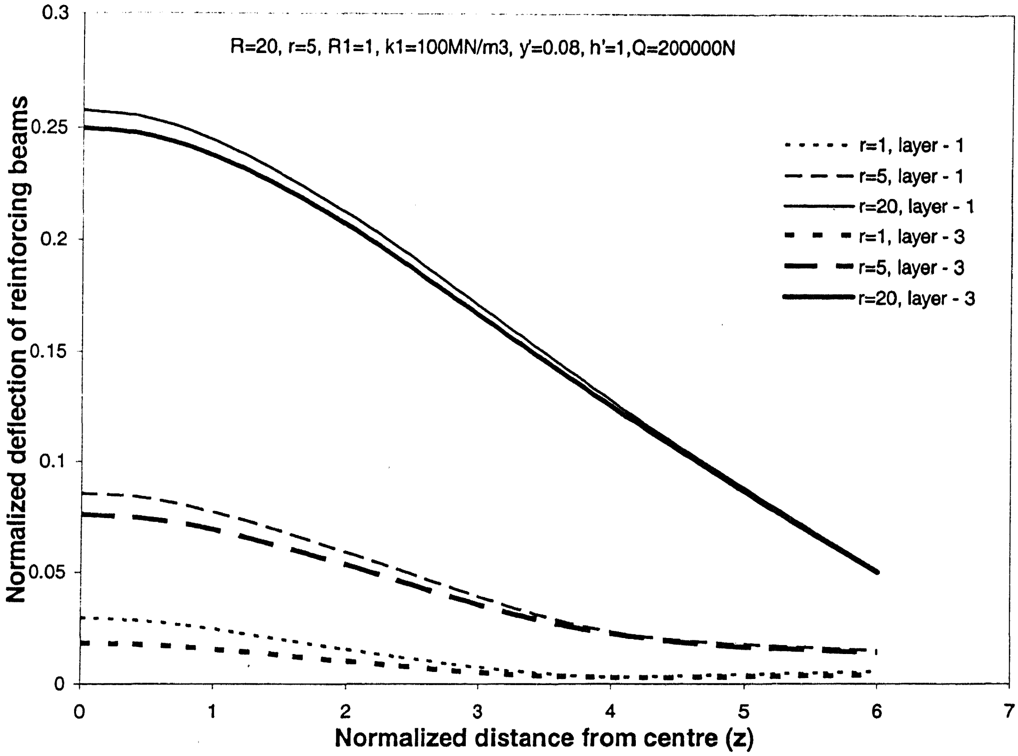


**Fig. 4.17: Normalized deflection of foundation beam for various values of *r* for load acting at the centre**

Fig. 4.18 shows that the maximum normalized deflections are found at the edges and it increase from 0.871 to 5.1 and minimum normalized deflection at the edge increases from 0.33 to 4.4 as *r* increases 1 to 20.

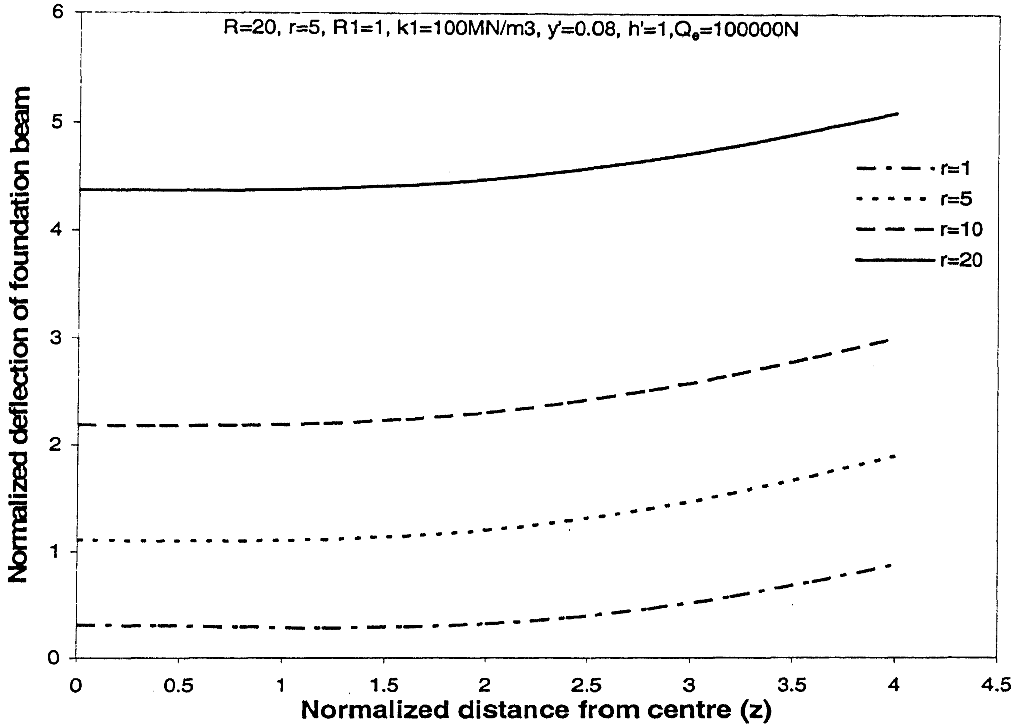


**Fig. 4.18: Normalized deflection of foundation beam for various values of *r* for loads acting at the edges**

From Fig. 4.19 it can be seen that the maximum deflection occurs at z = 3.6 of foundation beam and minimum settlement at the edge of reinforcing beam. It is also observed that for a typical value of ratio *r* layer one deflects more than the layer three. It shows that beam near to the foundation has greater effect. The maximum deflection increases 0.028 to 0.239 and 0.0163 to 0.229 for layer - 1 and layer -3 respectively as r increases from 1 to 20.

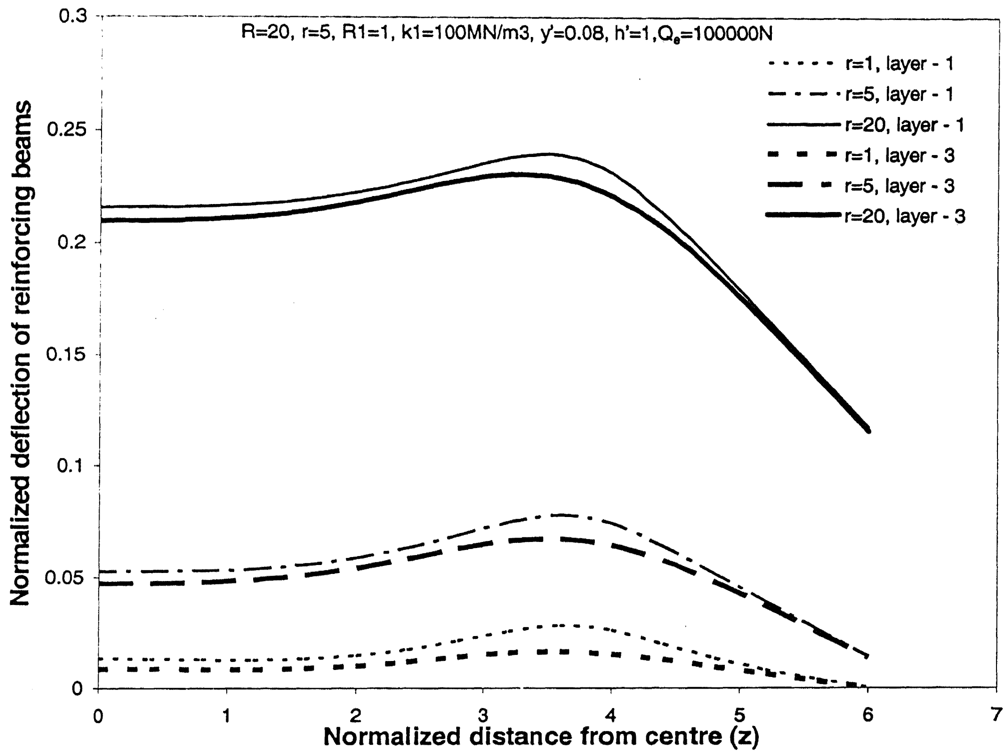


**Fig. 4.19: Normalized deflection of foundation beam for various values of *r* for loads acting at the edges**

## 4.4 Particular case of multiple layer reinforcement without reinforcement at interface

As a particular case of the above study, only one reinforcement layer is kept at the mid depth of dense compacted soil layer. This is simulated by analyzing the two layer reinforcement of the present model and keeping very low value of $E_2I_2$ very low i.e. of order $10^{-10}$ for the beam elements corresponding to the reinforcement at the interface of soil layers.

In Fig 4.20 and Fig 4.21, the deflection profiles for the foundation and the reinforcing beams are presented respectively for a set of typical values of parameters, showing the effect of reinforcement at the mid depth of dense compacted sand layer

for concentrated load acting at the center of the foundation beam. Figs. 4.22 and Fig. 4.23 show similar plots for the foundation beam subjected to end loads.

It is observed that the reduction in the maximum deflection of foundation beam is 20 % and 30 % with respect to unreinforced for load acting at centre and edge respectively.

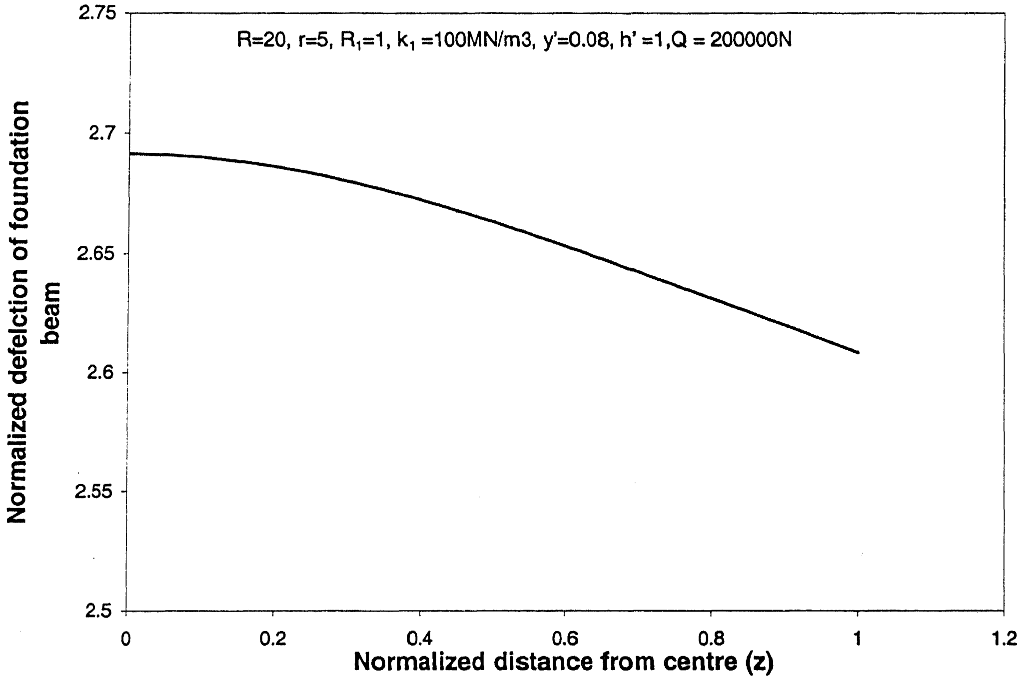


**Fig. 4.20: Normalized Deflection of foundation for reinforcement at the mid depth for load acting at the centre**

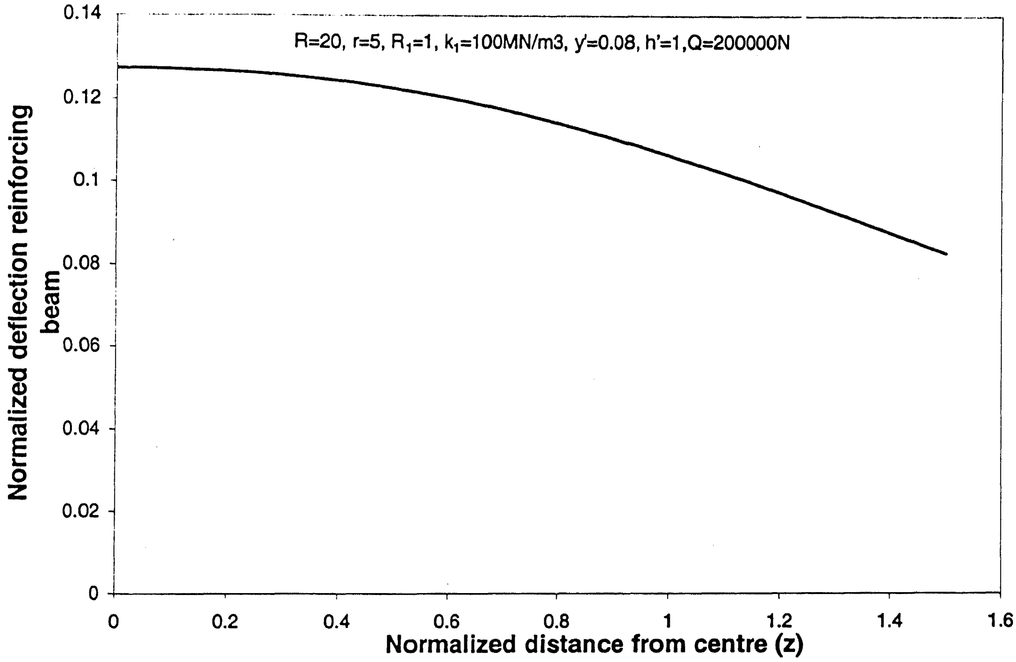


**Fig. 4.21: Normalized Deflection of reinforcement for reinforcement at the mid depth for load acting at the centre**

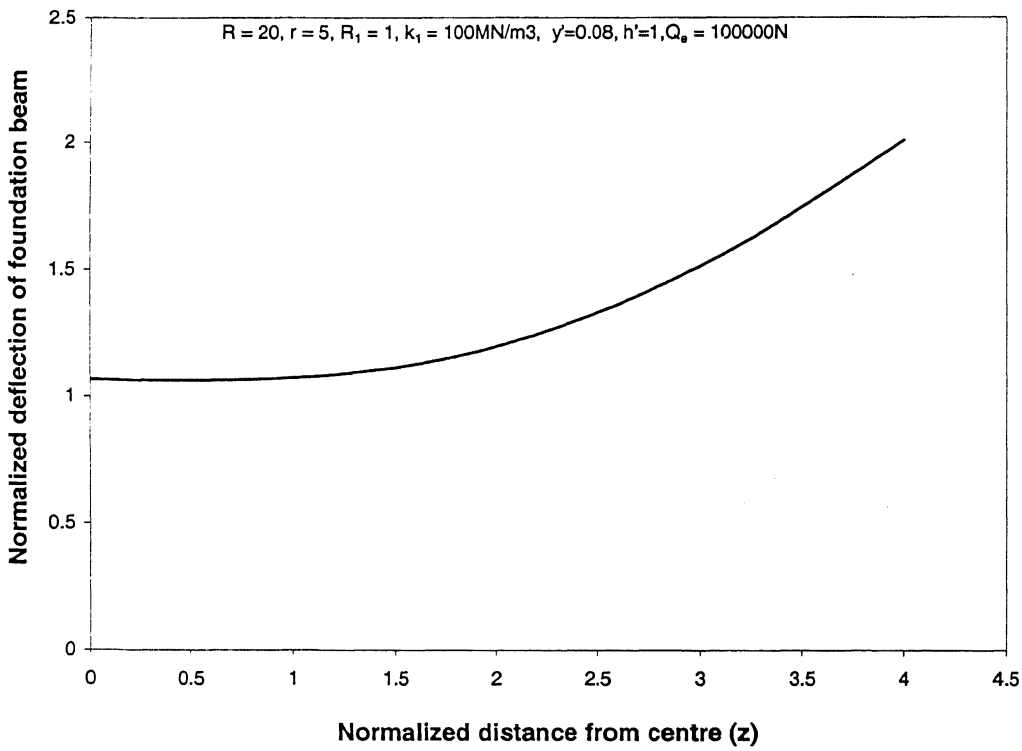


**Fig. 4.22: Normalized deflection of foundation for reinforcement at the mid depth for load acting at the edges**

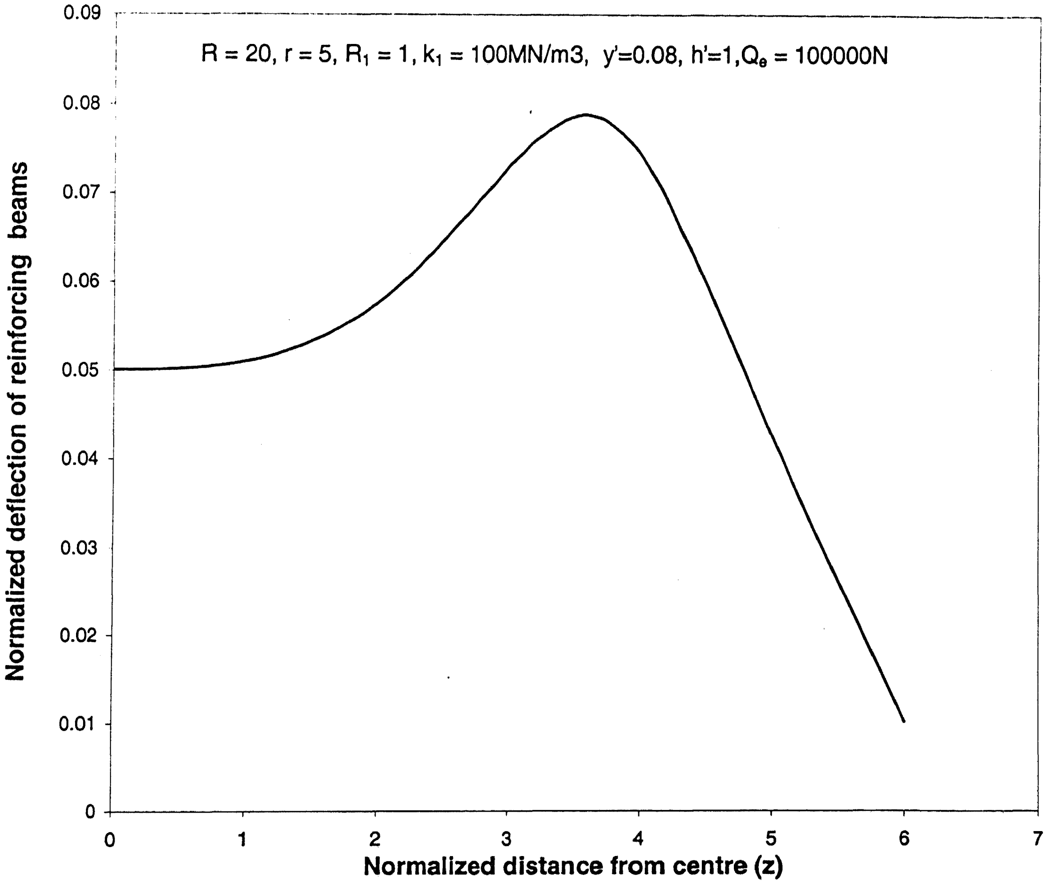


**Fig. 4.23: Normalized deflection of reinforcing beam for reinforcement at the mid depth for load acting at the edges**

# CHAPTER 5

# CONCLUSIONS AND SCOPE OF FUTURE STUDY

## 5.1 General

Following the problem formulation and method of analysis, multilayered reinforced earth foundation system is analyzed for the settlement response of foundation and reinforcing beams. The present model results are validated and then detailed results for parametric studies are obtained and discussed. Based on the results of the present model study following conclusions are drawn.

## 5.2 Conclusions

1. Results of the present model are compared with the close form solution by Maheshwari (2004) for a degenerated case. The present model results are in very good agreement with close form solution by Maheshwari (2004).
2. The number of layers of reinforcement significantly affects the settlement response of foundation beams for load acting at centre as well as at edges. The reduction in maximum normalized deflection for load acting at centre and for loads acting at the edges are 23 % and 35 % when three layer of reinforcements are used. Number of layers of reinforcement more than three does not have any significant effect on the settlement response of foundation and reinforcing beams for both the loading conditions.
3. The Load acting on the foundation beam affects the settlement response of both foundation and reinforcing beams significantly. For the load acting at center, the decrease in the maximum normalized deflection at the centre for

foundation beam and reinforcing beams is of the order of 75 % and 76 – 77 % when $\gamma'$ decreases from 1 to 0.05. For loads acting at edges, the decrease in the maximum normalized deflection of the foundation beam and reinforcing beams are 75 % and 78 – 80 % respectively as $\gamma'$ decreases from 1 to 0.05.

4. Normalized depth of placement affects the settlement response of foundation beam and reinforcing beams significantly for the both the loading conditions. For the load acting at centre the increase in maximum deflection at the centre for foundation beam and reinforcing beams is 26 % and 27 - 30 % when normalized depth of placement increases from 0.5 to 1.5. For the loads acting at the edges the maximum normalized deflection of foundation beam and reinforcing beams increases by 25 % and 32- 35 % respectively when normalized depth of placement increases from 0.5 to 1.5.
5. The relative flexural rigidity ratio $R$ affects the settlement response of foundation beam and reinforcing beams significantly for both the loadings. For the load acting at centre the maximum normalized deflection at the centre of foundation beam increases by 4 % when $R$ increases from 10 to 60. The maximum normalized deflection of reinforcing beams decreases by 60 – 90 % when $R$ increases from 10 to 60. For the loads acting at edges the increase in maximum deflection at the edge of foundation beam is 17 % when $R$ increases from 10 to 60 and the maximum normalized deflection of reinforcing beams decreases by 80 % when $R$ increases from 10 to 60.
6. The relative stiffness ratio $r$ of the soils affects the settlement response of foundation beam and reinforcing beams significantly for both the loading conditions. For the load acting at centre the increase in maximum normalized deflection at the centre of foundation beam and reinforcing beams are 650 %

and 700 % respectively when $r$ increases from 1 to 20. For the loads acting at edges the maximum normalized deflection of foundation beam increases by 485 % when $r$ increases from 1 to 20 respectively.

7. When only one layer of reinforcement is placed at the middle of compacted soil layer the reduction in maximum normalized deflection with respect to unreinforced earth is 20 % and 30 % for load acting at centre and loads acting at the edges respectively.

## 5.3 Scope of future study

Following are the future scopes of the present work

1. Higher order approximation for foundation beam and reinforcing beam are to be taken, $\frac{d^2y}{dx^2}$ and $\frac{d^3y}{dx^3}$ are to additional degrees of freedom so that shear force distribution and bending moment distribution on beams can be determined.
2. The present model results are to be validated by experiments.
3. Dynamic consideration is to be given to consider the inertial effect and study of moving loads.

# REFERENCES


1. Andrawes, K. Z., McGown, A., Wilson-Fahmy, R. F. and Mashhour, M. M. (1982) "The finite element method of analysis applied to soil-geotextile systems" *Second International Conference on Geotextiles, Las Vegas, U. S. A.*, pp. 695 – 700.
2. Binquet, J. and Lee, K. L. (1975) "Bearing capacity analysis of reinforced earth slabs" *Journal of Geotechnical Engineering Division, ASCE,* Vol. 101, No. GT12, pp. 1257 – 1276.
3. Brown, B. S. and Poulos, H. G. (1981) "Analysis of foundation on reinforced soil" *Proceedings of the Tenth International Conference on Soil Mechanics and Foundation Engineering, Stockholm, Sweden,* pp. 595 – 598.
4. Clough, Ray w., Joseph Penzien. (1993). *Dynamics of Structures.* McGraw Hill.
5. Mario Paz. (1987). *Structural Dynamics.* CBS.
6. Cook, Robert Davis (1981). *Concepts and Applications of Finite Element Analysis.* John Wiley.
7. Fakher, A. and Jones, C. J. F. P. (2001) "When bending stiffness of geosynthetics is important" *Geosynthetics International*, Vol. 8, No. 5, pp. 445 – 460.
8. Gharpure, A. (1995). "Finite Element Analysis of Geotextile Reinforced Sand-Bed Subjected to Strip Loading" *MTech. Thesis*, Dept. of Civil Engg, IIT Kanpur.
9. Ghosh, C. and Madhav, M. R. (1994a) "Settlement response of a reinforced shallow earth bed" *Geotextile and Geomembranes,* Vol. 13, pp. 643 – 656.
10. Ghosh, C. and Madhav, M. R. (1994b) "Reinforced granular fill-soft soil system: Confinement effect" *Geotextile and Geomembranes,* Vol. 13, pp. 727 – 741.

11. Ghosh, C. and Madhav, M. R. (1994c) "Reinforced granular fill-soft soil system: Membrane effect" *Geotextile and Geomembranes,* Vol. 13, pp. 743 – 759.

12. Madhav, M. R. and Poorooshasb, H. B. (1988) "A new model for geosynthetic reinforced soil" *Computers and Geotechnics*, Vol. 6, No. 4, pp. 277 – 290.

13. Maheshwari, P. (2004) "Response of reinforced granular bed soft soil system to static ad dynamic loads" *PhD. Thesis,* Department of Civil Engineering, Indian Institute of Technology, Kanpur, India.

14. Poran, C. J., Hermann, L. R. and Romstad, K. M. (1989) "Finite element analysis of footings on geogrid-reinforced sand" Geosynthetics Conference, San Diego, U. S. A., pp. 231 – 242.

15. Shukla, S. K. and Chandra, S. (1994a) "The effect of prestressing on settlement characteristics of geosynthetic-reinforced soil" *Geotextiles and Geomembranes,* Vol. 531 – 543.

16. Shukla, S. K. and Chandra, S. (1994b) "A study of settlement response of a geosynthetic-reinforced compressible granular fill-soft soil system" *Geotextile and Geomembranes,* Vol. 13, pp. 627 – 639.

17. Shukla, S. K. and Chandra, S. (1994c) "A generalized mechanical model for geosynthetic-reinforced foundation soil" *Geotextiles and Geomembranes*, Vol. 13, pp. 813 – 825.

18. Tirupathin R. Chandrapatla and Ashok D. Belegundu (2003). *Introduction to Finite Elemens inEngineering*. Prentice-Hall India.

19. Yin, J. H. (1997) "Modeling geosynthetic-reinforced granular fills over soft soil" *Geosynthetics International*, Vol. 4, No. 2, pp. 165 – 183.

20. Yin, J. H. (2000 ) “Close-form solution for reinforced Timoshenko beam on elastic foundation” *Journal of Engineering Mechanics Division, ASCE,* Vol. 126, No. 8, pp. 868 – 874.